Robust On-Off Pulse Control of Flexible Space Vehicles

Final Report of the Second-Year Project

RICIS Preface

This research was conducted under auspices of the Research Institute for Computing and Information Systems. Dr. Bong Wie of Arizona State University acted as Principal Investigator, with assistance from Ravi Sinha. Dr. A. Glen Houston served as RICIS research coordinator.

Funding was provided by the Engineering Directorate, NASA/JSC through Cooperative Agreement NCC 9-16 between the NASA Johnson Space Center and the University of Houston-Clear Lake. Dr. Kenneth J. Cox was the Division Chief of the Navigation Control and Aeronautics Division. The NASA research coordinator for this activity was Dr. John W. Sunkel, of the Navigation Control and Aeronautics Division, Engineering Directorate, NASA/JSC.

ABSTRACT

The on-off reaction jet control system is often used for attitude and orbital maneuvering of various spacecraft. Future space vehicles such as the orbital transfer vehicles, orbital maneuvering vehicles, and space station will extensively use reaction jets for orbital maneuvering and attitude stabilization. The proposed robust fuel- and time-optimal control algorithm is used for a three-mass spring model of flexible spacecraft. A fuel-efficient on-off control logic is developed for robust rest-to-rest maneuver of a flexible vehicle with minimum excitation of structural modes.

The first part of this report is concerned with the problem of selecting a proper pair of jets for practical trade-offs among the maneuvering time, fuel consumption, structural mode excitation, and performance robustness. A time-optimal control problem subject to parameter robustness constraints is formulated and solved.

The second part of this report deals with obtaining parameter insensitive fuel- and time-optimal control inputs by solving a constrained optimization problem subject to robustness constraints. It is shown that sensitivity to modeling errors can be significantly reduced by the proposed, robustified open-loop control approach.

The final part of this report deals with sliding mode control design for uncertain flexible structures. The benchmark problem of a flexible structure is used as an example for the feedback sliding mode controller design with bounded control inputs and robustness to parameter variations is investigated.

ACKNOWLEDGEMENTS

This research was supported by the NASA Johnson Space Center through the RICIS program of the University of Houston at Clear Lake. The authors would like to express special thanks to Dr. Kenneth Cox and Dr. John Sunkel of the NASA JSC for sponsoring this research.

TABLE OF CONTENTS

LIST OF TABLES

LIST OF FIGURES

Chapter 1

Introduction

In recent years there has been an interest in deployment of large space structures in earth's orbit for scientific and commercial activity. These large structures are required to be lightweight and are flexible compared to the bulky rigid structures which were deployed earlier. These flexible structures need active control to damp vibrations and to maintain figure. The design of control systems for such an application using nonlinear control elements like an on-off thruster is a different problem. One problem is controlling these structures for rest-to-rest maneuver in minimum time. The well known standard problem of bang-bang control has been solved using the minimum principle in [1]. The requirement of time minimization results in bang-bang or pulsed one sided control which can be implemented using current on-off actuation technology. Another problem would be to minimize a performance index which weighs time against fuel consumption for a rest-to-rest maneuver. This is a more difficult problem for trajectories originating from the same point which satisfy the first order necessary conditions are not unique. Further, the control system should be robust to uncertainty in modeling which would occur due to parameter varations. The total inertia of the flexible structure is well known but there is uncertainty in the mass distribution and stiffness of the flexible structure. These parameter variations has been shown to create residual vibration during and/or after maneuver. The problem is of selecting a proper pair of jets for practical trade-offs

among maneuvering time, fuel consumption, structural mode excitation, and performance robustness is studied. Open-loop study of robust fuel- and time-optimal control gives insight into the characterstics of control structures which optimizes manuevering time and fuel consumption. Such controls would be desirable in closed-loop control system designed to reduce the effect of disturbances and parameter variations. The ultimate goal of the future is to develop nonlinear feedback control logic for achieving the robust fuel- and time-optimal performance. Most robust linear feedback controllers do not fully utilize the available control power in performing a time-optimal maneuver. An attempt is made to use the sliding mode control technique to obtain a fast settling time and be robust to parameter variations using bounded control inputs.

The minimum time problem for flexible spacecraft has been addressed in several technical papers [2,3,4,5]. In [3], the bang-bang control is shown to have an odd number of switches and to be an odd function of time about the middle switch. In [3,4,5] statements are made that "in most cases" the time-optimal control for a rigid body and n bending modes has $2n + 1$ switches. In [6] it is proved that when $n = 1$, there are never more than three switches for scalar control. In [7] an optimal open-loop control is obtained for fixed maneuver time where the intermediate switching time is selected to minimize the post-maneuver energy. In [14,15] near-optimal maneuvers to perform the retargetings, which minimize fuel consumption, were also obtained. In minimizing settling time, it is shown that time-optimal control is sensitive to parameter variations. The residual vibrations occurs as a result of parameter variations. In [10] forcing functions are constructed which attenuate residual vibrations. In [8] a finite Fourier expansion for the forcing function is used and coefficients are picked in such a way so as to reduce the peaks of the frequency spectrum at discrete points. This only eliminates a few of the peaks and leaves some

modes excited. However this is not time-optimal forcing function. In [9] an appropriately shaped torque is derived which not only minimizes residual vibrations but also minimizes the effect of parameter variations which change the modal frequencies. These methods use a smooth continuous forcing functions having initial and final zero slopes so that the structural modes are not excited. But our results show to contrary that the proper sequence of on-off pulse are required.

The sliding mode control theory has been studied in great detail in [24]. This nonlinear feedback control is used to achieve accurate tracking in presence of disturbance and parameter variations. In [22] continuous control laws are incorporated to approximate the idealized sliding mode control. This eliminates chattering, the high frequency component of control which occurs in idealized sliding mode control. However, these schemes do not use bounded control inputs.

In this thesis the primary objective is to study the feasibility of computing open-loop on-off pulse control logic for uncertain spacecraft. The robust time-optimal control which brings the flexible spacecraft from rest-to-rest maneuver are obtained. The lumped mass spring model with negligible damping is used as a model of a flexible spacecraft. A constrained parameter optimization approach is used to solve this problem. The theoretical and practical implementation issues inherent to constrained optimization are not elaborated. The bang-bang control and one sided control inputs are obtained. The one-sided control need not be an odd function about mid maneuver time and it becomes a difficult problem to solve than the standard problem. Many theoretical issues (i.e. uniqueness and structure of time-optimal) needs to be resolved. It is shown that an accurate mathematical modeling is required for time-optimal solution

and that they are sensitive to modeling uncertainty. The parameter optimization problem is formulated and solved with additional robustness constraints. Because of properly coordinated pulse sequences the flexible modes are not significantly excited during maneuver and the residual response after the maneuver are well desensitized. The two one-sided controls show "bang-off-bang" nature in the time optimal solution. This motivates the problem of computing the on-off control logic for fuel- and time-optimal control of a flexible spacecraft which is generally a difficult problem to solve. The mass spring model with one/two flexible modes are used as examples of flexible spacecraft. The sensitivity to parameter variations is reduced by using robustness constraints. The feedback control method of sliding mode control design for uncertain flexible structure for benchmark problem using bounded control inputs is presented. The robustness to parameter variations is illustrated for this design.

The remainder of this thesis is organized as follows. Chapter 2 deals with the robust time-optimal control of uncertain spacecraft. In chapter 3, the robust fuel- and time-optimal control of uncertain flexible spacecraft is presented. Chapter 4 presents the detailed review of the sliding control theory and its application to the benchmark problem of flexible spacecraft. Chapter 5 is the conclusion. Appendix A reviews the numerical solution of nonlinear constrained optimization problem.

Chapter 2

Robust Time-Optimal Control of Uncertain Flexible Spacecraft

2.1 Introduction

This chapter deals with the problem of computing open-loop, on-off jet firing logic for flexible spacecraft which are sometimes required to maneuver as quickly as possible with a minimum of structural vibrations during and/or after a maneuver. Most standard time-optimal control approaches to such a problem require an accurate mathematical model, and thus the resulting solution becomes sensitive to variations in model parameters.

Expanding on the recent results of [11,12], we further explore the robust time-optimal control problem of flexible spacecraft in the face of modeling uncertainty. In particular, we study the problem of selecting a proper pair of jets for practical trade-offs among the maneuvering time, fuel consumption, structural mode excitation, and performance robustness. A parameter optimization approach, with additional constraints for performance robustness with respect to modeling uncertainty, is employed to solve such a robust time-optimal control problem. However, many theoretical and practical implementation issues inherent to constrained parameter optimization problems are not elaborated in this chapter.

A simple math model of flexible spacecraft with a rigid-body mode and two flexible modes, as shown in Fig. 2.1, is used to illustrate the concept and

methodology. We consider the case in which the structural flexibility and mass distribution of the vehicle are quite uncertain, while the total mass (or inertia) of the vehicle is well known. Consequently, we focus on the robust control problem of flexible spacecraft in the face of modal frequency uncertainty as well as mode shape uncertainty.

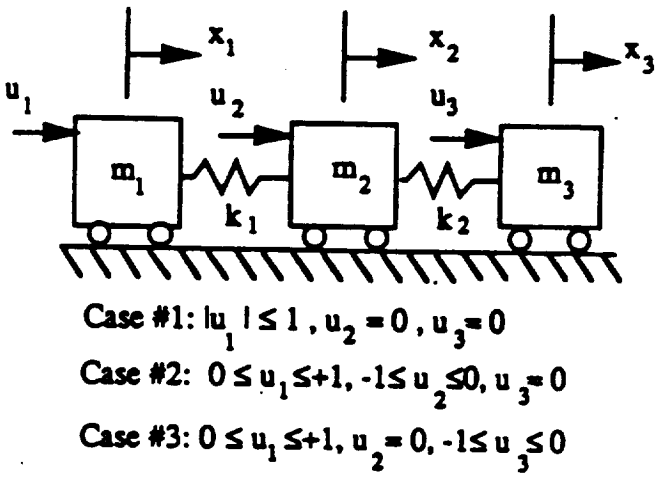

Figure 2.1: Three-mass-spring dynamical system.

Other robustified, open-loop approaches, however, attempt to find a smooth continuous forcing function (e.g., a versine function) that begins and ends with zero slope. The basic idea behind such approaches is that a smooth control input without sharp transitions is less likely to excite structural modes during maneuvers. On the contrary to such a common notion, the results of this chapter indicate that properly modulated, on-off pulse sequences can achieve a fast maneuvering time with a minimum of structural vibrations during and/or

after a maneuver, even in the face of plant modeling uncertainty.

The remainder of this chapter is organized as follows. Section 2.2 describes the standard time-optimal control problem of flexible spacecraft without modeling uncertainty. A parameter optimization problem is formulated, in which the objective function is the maneuvering time. Three cases are explored, as illustrated in Fig. 2.1, in order to assess the actuator placement problem for time-optimal control of flexible spacecraft with multiple jets. In Section 2.3, we investigate the same problem as in Section 2.2 but considering the presence of modeling uncertainty. A time-optimal control problem subject to additional robustness (or sensitivity) constraints is formulated, and numerical solutions for three cases are then compared with solutions obtained in Section 2.2.

2.2 Time-Optimal Rest-to-Rest Maneuver Control

2.2.1 Problem Formulation

Consider a flexible spacecraft described by

$$M\ddot{x} + Kx = Gu \tag{2.1}$$

where x is a generalized displacement vector, M a mass matrix, K a stiffness matrix, G the control input distribution matrix, and u the control input vector.

Equation (2.1) is transformed into the modal equations:

$$\begin{aligned} \ddot{y}_1 + \omega_1^2 y_1 &= \phi_{11}u_1 + \phi_{12}u_2 + \phi_{13}u_3 \\ \ddot{y}_2 + \omega_2^2 y_2 &= \phi_{21}u_1 + \phi_{22}u_2 + \phi_{23}u_3 \\ &\vdots \\ \ddot{y}_n + \omega_n^2 y_n &= \phi_{n1}u_1 + \phi_{n2}u_2 + \phi_{n3}u_3 \end{aligned} \tag{2.2}$$

where y_i is the i^{th} modal coordinate, ω_i the i^{th} modal frequency, ϕ_{ij} the modal input distribution coefficient, and n the number of modes considered in control

design. Without loss of generality, only three control inputs are considered in Eq. (2.2).

In this chapter, we consider a simple model which is a generic representation of a spacecraft with a rigid-body mode and two flexible modes, as shown in Fig. 2.1. Three cases are studied: (i) Case 2-1 with both "positive" and "negative" jets placed at body 1, (ii) Case 2-2 with a "positive" jet at body 1 and a "negative" jet at body 2, and (iii) Case 2-3 with a "positive" jet at body 1 and a "negative" jet at body 3. Case 2-1 is a typical case in which two opposing jets are colocated. In Cases 2-2 and 2-3, two opposing jets are not colocated.

For a class of problems, such as Case 2-1; the modal equations become

$$\ddot{y}_i + \omega_i^2 y_i = \phi_i u; \quad i = 1, \cdots, n \tag{2.3}$$

where ϕ_i the i^{th} modal gain and the scalar control input u is bounded as

$$-1 \leq u \leq 1 \tag{2.4}$$

The problem is to find the control input $u(t)$ which minimizes the performance index

$$J = \int_0^{t_f} dt = t_f$$

subject to Eqs. (2.3) and (2.4), and given boundary conditions. The time-optimal bang-bang solution of this problem with the rest-to-rest maneuvering boundary conditions has, in most cases, $(2n-1)$ switches, and the solution is symmetric about the mid-maneuver time $t_f/2$ [12]. That is, for a case with $(2n-1)$ switches, we have the symmetric switching pattern given as:

$$t_j = t_{2n} - t_{2n-j}; \qquad j = 1, \cdots, n \tag{2.5}$$

where t_j is the j^{th} switching time and $t_{2n} = t_f$.

A bang-bang input with $(2n-1)$ switches is expressed as

$$u(t) = \sum_{j=0}^{2n} B_j u_s(t - t_j) \tag{2.6}$$

where B_j is the magnitude of a unit step function $u_s(t)$ at t_j. This function can be characterized by its switch pattern as:

$$B = \{ B_0, \quad B_1, \quad B_2, \cdots, B_{2n} \}$$
$$T = \{ t_0, \quad t_1, \quad t_2, \cdots, t_{2n} \}$$

where B represents a set of B_j with $B_0 = B_{2n} = \pm 1$ and $B_j = \pm 2$ for $j = 1, \cdots, 2n-1$; T represents a set of switching times $(t_1, \cdots, t_{2n-1})$ and the initial and final times ($t_0 = 0$ and $t_f = t_{2n}$).

The rest-to-rest maneuvering constraint for the rigid-body mode ($\omega_1 = 0$) can be found as

$$\frac{\phi_1}{2} \sum_{j=0}^{2n} (t_f - t_j)^2 B_j - y_1(t_f) = 0 \tag{2.7}$$

The i^{th} structural mode solution for the control input of Eq. (2.6) for $t \geq t_f$ is

$$\begin{aligned} y_i(t) &= -\frac{\phi_i}{\omega_i^2} \sum_{j=0}^{2n} B_j \cos\omega_i(t - t_j) \\ &= -\frac{\phi_i}{\omega_i^2} [\cos\omega_i(t - t_n) \sum_{j=0}^{2n} B_j \cos\omega_i(t_j - t_n) \\ &\quad + \sin\omega_i(t - t_n) \sum_{j=0}^{2n} B_j \sin\omega_i(t_j - t_n)] \end{aligned} \tag{2.8}$$

and it can be shown that the following constraint equation for each mode

$$\sum_{j=0}^{2n} B_j \sin\omega_i(t_j - t_n) = 0 \tag{2.9}$$

is always satisfied for any bang-bang input which is symmetric about the mid-maneuver time t_n. Consequently, we have the following flexible mode constraints for no-residual structural vibration (i.e., $y_i(t) = 0$ for $t \geq t_f$):

$$\sum_{j=0}^{2n} B_j \cos \omega_i (t_j - t_n) = 0 \tag{2.10}$$

for each flexible mode.

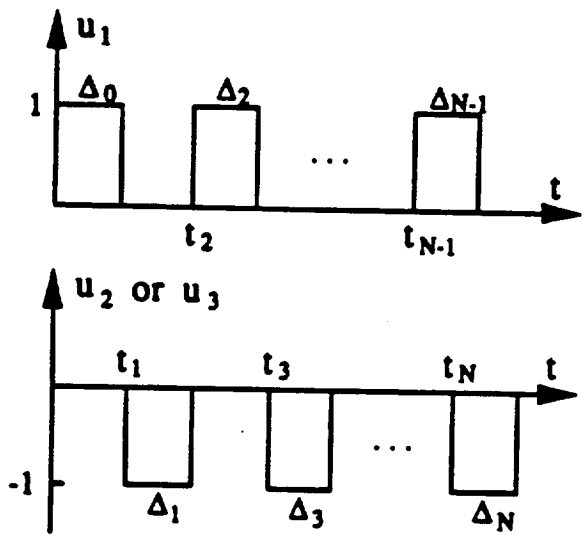

Figure 2.2: Pulse sequences.

On the other hand, for Case 2-2 with the pulse sequences as illustrated in Fig. 2.2, the boundary conditions of the rest-to-rest maneuvering problem result in the following constraint:

$$\phi_{11} \sum_{j=0,2}^{N-1} \Delta_j - \phi_{12} \sum_{j=1,3}^{N} \Delta_j = 0 \tag{2.11}$$

where ϕ_{11} and ϕ_{12} are the modal input distribution coefficients associated with the rigid-body mode and the two control inputs u_1 and u_2, and Δ_j and N are defined as in Fig. 2.2.

The positioning constraint for the rigid-body mode, with specified $y_1(t \geq t_f)$, then becomes

$$\begin{aligned} 2y_1(t_f) \;-\; & \phi_{11} \sum_{j=0,2}^{N-1} [2t_j\Delta_j + \Delta_j^2] \\ +\; & \phi_{12} \sum_{j=1,3}^{N} [2t_j\Delta_j + \Delta_j^2] = 0 \end{aligned} \tag{2.12}$$

Also, rest-to-rest maneuvering requires that for each flexible mode, $y_i(t) = 0$ for $t \geq t_f$; i.e., we have

$$-\phi_{i1} \sum_{j=0,2}^{N-1} c_{ij} + \phi_{i2} \sum_{j=1,3}^{N} c_{ij} = 0 \tag{2.13}$$

$$\phi_{i1} \sum_{j=0,2}^{N-1} s_{ij} - \phi_{i2} \sum_{j=1,3}^{N} s_{ij} = 0 \tag{2.14}$$

where

$$\begin{aligned} c_{ij} &= \cos(\omega_i t_j) - \cos(\omega_i(t_j + \Delta_j)) \\ s_{ij} &= \sin(\omega_i t_j) - \sin(\omega_i(t_j + \Delta_j)) \end{aligned}$$

for $i = 2, \cdots, n$.

Remark: For cases in which the control inputs are one-sided, each control input for the time-optimal solution need not be an odd function about the mid-maneuver time. Thus, the problem with one-sided control inputs becomes more difficult to solve than the standard problem with two-sided control inputs, and many theoretical issues (e.g., the uniqueness and structure of time-optimal solutions) need to be resolved. We now present a detailed solution of each case.

2.2.2 Case 2-1 with a Two-Sided Control Input

In this case, as illustrated in Fig. 2.1, a two-sided control input is bounded as:

$$-1 \leq u(t) \leq +1$$

and the equations of motion for this case are

$$\begin{aligned} m_1\ddot{x}_1 + k_1(x_1 - x_2) &= u \\ m_2\ddot{x}_2 + k_1(x_2 - x_1) + k_2(x_2 - x_3) &= 0 \\ m_3\ddot{x}_3 + k_2(x_3 - x_2) &= 0 \end{aligned}$$

where x_1, x_2 and x_3 are the positions of body 1, body 2 and body 3, respectively, and the nominal parameters are $m_1 = m_2 = m_3 = k_1 = k_2 = 1$ with appropriate units and time is in units of second.

The boundary conditions for a rest-to-rest maneuver are given as

$$x_1(0) = x_2(0) = x_3(0) = 0 \tag{2.15}$$

$$x_1(t_f) = x_2(t_f) = x_3(t_f) = 1 \tag{2.16}$$

$$\dot{x}_1(0) = \dot{x}_2(0) = \dot{x}_3(0) = 0 \tag{2.17}$$

$$\dot{x}_1(t_f) = \dot{x}_2(t_f) = \dot{x}_3(t_f) = 0 \tag{2.18}$$

The modal equations are

$$\ddot{y}_1 = 0.3333u \tag{2.19}$$

$$\ddot{y}_2 + \omega_2^2 y_2 = 0.5u \tag{2.20}$$

$$\ddot{y}_3 + \omega_3^2 y_3 = -0.1667u \tag{2.21}$$

where

$$\omega_2^2 = [-b - \sqrt{b^2 - 4k_1k_2\,c}]/2 \tag{2.22}$$

$$\omega_3^2 = [-b + \sqrt{b^2 - 4k_1k_2\,c}]/2 \tag{2.23}$$

$$b = \frac{-k_1(m_1+m_2)m_3 - k_2(m_2+m_3)m_1}{m_1m_2m_3} \tag{2.24}$$

$$c = (m_1+m_2+m_3)/(m_1m_2m_3) \tag{2.25}$$

and $\omega_2 = 1$ rad/sec and $\omega_3 = \sqrt{3}$ rad/sec for the nominal system. The corresponding boundary conditions for the modal coordinates are

$$y_1(0) = y_2(0) = y_3(0) = 0 \tag{2.26}$$

$$y_1(t_f) = 1, \;\; y_2(t_f) = y_3(t_f) = 0 \tag{2.27}$$

$$\dot{y}_1(0) = \dot{y}_2(0) = \dot{y}_3(0) = 0 \tag{2.28}$$

$$\dot{y}_1(t_f) = \dot{y}_2(t_f) = \dot{y}_3(t_f) = 0 \tag{2.29}$$

The time-optimal control input with 5 switches is expressed as

$$\begin{aligned} u(t) &= u_s(t) - 2u_s(t-t_1) + 2u_s(t-t_2) - 2u_s(t-t_3) \\ &+ u_s(t-t_4) - u_s(t-t_5) + u_s(t-t_6) \end{aligned} \tag{2.30}$$

with the symmetry conditions

$$\begin{aligned} t_6 &= 2t_3 \\ t_5 &= 2t_3 - t_1 \\ t_4 &= 2t_3 - t_2 \end{aligned}$$

The time-optimal control problem is then formulated as the following constrained minimization problem:

$$min\ J = t_f = t_6 = 2t_3 \tag{2.31}$$

subject to the following constraints:

$$6 - t_6^2 + \sum_{j=1}^{5}(-1)^{j+1}[2(t_6 - t_j)^2] = 0 \tag{2.32}$$

$$1 + \cos(\omega_2 t_3) + 2\sum_{j=1}^{2}(-1)^j \cos(\omega_2(t_3 - t_j)) = 0 \tag{2.33}$$

$$1 + \cos(\omega_3 t_3) + 2\sum_{j=1}^{2}(-1)^j \cos(\omega_3(t_3 - t_j)) = 0 \tag{2.34}$$

$$t_1,\ t_2,\ t_3 > 0 \tag{2.35}$$

A numerical technique of nonlinear constrained optimization problem discussed in Appendix A, was used to obtain a solution as:

$$\begin{aligned} u(t) &= u_s(t) - 2u_s(t - 0.944) + 2u_s(t - 2.012) \\ &- 2u_s(t - 3.255) + u_s(t - 4.499) \\ &- u_s(t - 5.567) + u_s(t - 6.511) \end{aligned} \tag{2.36}$$

The time responses of x_3 to this time-optimal control input are shown in Fig. 2.3 for four different values of $k = k_1 = k_2$. We notice that the responses are quite sensitive to variations in the model parameters. Similar responses can also be observed for arbitrarily combined variations of k_i and m_i, but keeping the total mass constant ($m_1 + m_2 + m_3 = 3$). For convenience, simulation results only for $k = k_1 = k_2$ variations are presented in this chapter.

2.2.3 Case 2-2 with Two One-Sided Control Inputs

For Case 2-2, as illustrated in Fig. 2.1, two one-sided control inputs are bounded as

$$0 \leq \ u_1 \ \leq +1 \tag{2.37}$$

$$-1 \leq \ u_2 \ \leq 0 \tag{2.38}$$

For this case, the time-optimal control inputs are assumed as:

$$u_1 \ = \ u_s(t) - u_s(t - \Delta_0)$$

$$+ \quad u_s(t-t_2) - u_s(t-t_2-\Delta_2) \tag{2.39}$$

$$u_2 = -u_s(t-t_1) + u_s(t-t_1-\Delta_1)$$

$$- \quad u_s(t-t_3) + u_s(t-t_3-\Delta_3) \tag{2.40}$$

The modal equations for this case are

$$\ddot{y}_1 = 0.3333u_1 + 0.3333u_2 \tag{2.41}$$

$$\ddot{y}_2 + \omega_2^2 y_2 = 0.5u_1 \tag{2.42}$$

$$\ddot{y}_3 + \omega_3^2 y_3 = 0.1667u_1 - 0.3333u_2 \tag{2.43}$$

and the rest-to-rest maneuver constraints are

$$\Delta_0 - \Delta_1 + \Delta_2 - \Delta_3 = 0 \tag{2.44}$$

$$6 + \sum_{j=0}^{3}(-1)^j[\Delta_j^2 + 2t_j\Delta_j^2] = 0 \tag{2.45}$$

$$\sum_{j=0,2}[\cos(\omega_2 t_j) - \cos(\omega_2(t_j+\Delta_j))] = 0 \tag{2.46}$$

$$\sum_{j=0,2}[\sin(\omega_2 t_j) - \sin(\omega_2(t_j+\Delta_j))] = 0 \tag{2.47}$$

$$2\sum_{j=1,3}[\cos(\omega_3 t_j) - \cos(\omega_3(t_j+\Delta_j))]$$

$$+ \sum_{j=0,2}[\cos(\omega_3 t_j) - \cos(\omega_3(t_j+\Delta_j))] = 0 \tag{2.48}$$

$$2\sum_{j=1,3}[\sin(\omega_3 t_j) - \sin(\omega_3(t_j+\Delta_j))]$$

$$+ \sum_{j=0,2}[\sin(\omega_3 t_j) - \sin(\omega_3(t_j+\Delta_j))] = 0 \tag{2.49}$$

The time-optimal solution can then be obtained by solving the constrained minimization problem:

$$min\ J = t_f = t_3 + \Delta_3 \tag{2.50}$$

subject to the constraint given by Eqs. (2.49).

A solution of this problem can be found as

$$\begin{array}{ll} t_0 = 0.0000, & \Delta_0 = 1.0429 \\ t_1 = 1.9581, & \Delta_1 = 1.2401 \\ t_2 = 3.1416, & \Delta_2 = 1.0429 \\ t_3 = 4.504, & \Delta_3 = 0.8457 \\ t_f = 5.349 & \end{array} \tag{2.51}$$

The time responses of x_3 to the time-optimal control inputs are shown in Fig. 2.4 for four different values of $k = k_1 = k_2$. Similar to Case 2-1, the responses are sensitive to variations in the model parameters. An interesting feature of this case is that the pulse sequences are of a "bang-off-bang" type, resulting in the control on-time of 4.172 sec, which is different from the maneuver time of 5.35 sec.

2.2.4 Case 2-3 with Two One-Sided Control Inputs

For Case 2-3, as illustrated in Fig. 2.1, two one-sided control inputs are bounded as

$$0 \leq \quad u_1 \quad \leq +1 \tag{2.52}$$

$$-1 \leq \quad u_3 \quad \leq 0 \tag{2.53}$$

Similar to Case 2-2, the time-optimal control inputs are assumed as:

$$\begin{aligned} u_1 &= u_s(t) - u_s(t - \Delta_0) \\ &+ u_s(t - t_2) - u_s(t - t_2 - \Delta_2) \end{aligned} \tag{2.54}$$

$$\begin{aligned} u_3 &= -u_s(t - t_1) + u_s(t - t_1 - \Delta_1) \\ &- u_s(t - t_3) + u_s(t - t_3 - \Delta_3) \end{aligned} \tag{2.55}$$

The modal equations for this case are

$$\tilde{y}_1 = 0.3333(u_1 + u_3) \tag{2.56}$$

$$\ddot{y}_2 + \omega_2^2 y_2 = 0.5(u_1 - u_3) \tag{2.57}$$

$$\ddot{y}_3 + \omega_3^2 y_3 = 0.1667(u_1 + u_3) \tag{2.58}$$

and the rest-to-rest maneuver constraints are

$$\Delta_0 - \Delta_1 + \Delta_2 - \Delta_3 = 0 \tag{2.59}$$

$$6 + \sum_{j=0}^{3}(-1)^j[\Delta_j^2 + 2t_j\Delta_j^2] = 0 \tag{2.60}$$

$$\sum_{j=0}^{3}(-1)^j[\sin(\omega_2 t_j) - \sin(\omega_2(t_j + \Delta_j))] = 0 \tag{2.61}$$

$$\sum_{j=0}^{3}(-1)^j[\cos(\omega_2 t_j) - \cos(\omega_2(t_j + \Delta_j))] = 0 \tag{2.62}$$

$$\sum_{j=0}^{3}(-1)^j[\sin(\omega_3 t_j) - \sin(\omega_3(t_j + \Delta_j))] = 0 \tag{2.63}$$

$$\sum_{j=0}^{3}(-1)^j[\cos(\omega_3 t_j) - \cos(\omega_3(t_j + \Delta_j))] = 0 \tag{2.64}$$

$$t_1, t_2, t_3, t_4, t_5 > 0; \quad t_0 = 0$$

$$\Delta_j \geq 0$$

The time-optimal solution can then be obtained by solving the constrained minimization problem:

$$min\ J = t_f = t_3 + \Delta_3 \tag{2.65}$$

subject to the constraints given by Eqs. (2.64).

A solution of this problem is

$$\begin{array}{ll} t_0 = 0.0000, & \Delta_0 = 0.9510 \\ t_1 = 1.3631, & \Delta_1 = 0.1658 \\ t_2 = 2.8329, & \Delta_2 = 0.1658 \\ t_3 = 3.4109, & \Delta_3 = 0.9510 \\ t_f = 4.3619 & \end{array} \tag{2.66}$$

The time responses of x_3 to the time-optimal control inputs are shown in Fig. 2.5 for four different values of $k = k_1 = k_2$. Again, the responses are

quite sensitive to variations in the model parameters. Similar to Case 2-2, an interesting feature of this case is that the pulse sequences are of a "bang-off-bang" type, resulting in the control on-time of 2.234 sec, which is different from the maneuver time of 4.362 sec.

Compared to Case 2-1 and Case 2-2, this case has the fastest maneuver time as well as the smallest control on-time. Therefore, the actuator configuration of Case 2-3 can be considered to be "optimal" in the sense of minimizing both the maneuver time and the jet on-time.

2.3 Robust Time-Optimal Control

As shown in the preceding section, a standard, time-optimal control approach requires an accurate mathematical model and thus the resulting solution is often sensitive to plant modeling uncertainty.

In this section, expanding on the approach introduced in Section 2.2, a parameter optimization problem is formulated with additional constraints for robustness with respect to the structural frequency uncertainty. The resulting *robustified* or *desensitized*, time-optimal soultion is a multi-switch bang-bang control, and is thus implementable for spacecraft equipped with on-off reaction jets [13].

2.3.1 Problem Formulation

By taking the derivative of Eq. (2.8) with respect to ω_i, we get

$$\frac{dy_i(t)}{d\omega_i} = \frac{\phi_i}{\omega_i^2}\cos\omega_i(t-\frac{t_f}{2})\sum_{j=0}^{2n}(t_j-\frac{t_f}{2})B_j\sin\omega_i(t_j-\frac{t_f}{2}) \qquad (2.67)$$

for each flexible mode. Letting $dy_i(t)/d\omega_i = 0$ for all $t \geq t_f$, we have

$$\sum_{j=0}^{2n}(t_j - \frac{t_f}{2})B_j \cos\omega_i(t_j - \frac{t_f}{2}) = 0;\ i = 2, \cdots, n \tag{2.68}$$

which are called the first-order robustness constraints for the case with a two-sided control input.

Similarly, the robustness constraints for a case with two one-sided control inputs can be found as:

$$-\phi_{i1}\sum_{j=0,2}^{N-1} c_{ij} + \phi_{i2}\sum_{j=1,3}^{N} c_{ij} = 0 \tag{2.69}$$

$$\phi_{i1}\sum_{j=0,2}^{N-1} s_{ij} - \phi_{i2}\sum_{j=1,3}^{N} s_{ij} = 0 \tag{2.70}$$

where

$$c_{ij} = t_j \cos(\omega_i t_j) - (t_j + \Delta_j)\cos(\omega_i(t_j + \Delta_j))$$

$$s_{ij} = t_j \sin(\omega_i t_j) - (t_j + \Delta_j)\sin(\omega_i(t_j + \Delta_j))$$

which are called the first-order robustness constraints for the case with two one-sided control inputs.

2.3.2 Case 2-1 with a Two-Sided Control Input

For Case 2-1, the time-optimal control is a five-switch bang-bang function, but the resulting responses were shown to be very sensitive to variations in model parameters. A robustified, time-optimal solution of the same problem is now computed as follows. The robust time-optimal control input is assumed as:

$$u(t) = u_s(t) + 2\sum_{j=1}^{9}[(-1)^j u_s(t - t_j)] + u_s(t - t_{10}) \tag{2.71}$$

with the symmetry conditions

$$\begin{aligned} t_6 &= 2t_5 - t_4 \\ t_7 &= 2t_5 - t_3 \\ t_8 &= 2t_5 - t_2 \\ t_9 &= 2t_5 - t_1 \\ t_{10} &= 2t_5 \end{aligned} \tag{2.72}$$

The constrained optimization problem with the first-order robustness constraint can be formulated as:

$$min\ J = t_f = t_{10} \tag{2.73}$$

subject to

$$6 + \sum_{j=1}^{9}(-1)^{j+1}[2(t_{10} - t_j)^2] - t_{10}^2 = 0$$

$$1 + \cos(\omega_2 t_5) + 2\sum_{j=1}^{4}[(-1)^j \cos(\omega_2(t_j - t_5))] = 0$$

$$1 + \cos(\omega_3 t_5) + 2\sum_{j=1}^{4}[(-1)^j \cos(\omega_3(t_j - t_5))] = 0$$

$$t_5 \sin(\omega_2 t_5) + 2\sum_{j=1}^{4}(-1)^j (t_j - t_5)\sin(\omega_2(t_j - t_5)) = 0$$

$$t_5 \sin(\omega_3 t_5) + 2\sum_{j=1}^{4}(-1)^j (t_j - t_5)\sin(\omega_3(t_j - t_5)) = 0$$

$$t_1, t_2, t_3, t_4, t_5 > 0; \quad t_0 = 0$$

A robust time-optimal solution with 9 switches can be found as:

$$\begin{aligned} t_1 &= 0.560, \quad t_2 = 1.460 \\ t_3 &= 2.690, \quad t_4 = 3.804 \\ t_5 &= 5.091, \quad t_6 = 6.377 \\ t_7 &= 7.491, \quad t_8 = 8.722 \\ t_9 &= 9.622, \quad t_{10} = 10.18 \end{aligned} \tag{2.74}$$

The time responses of x_3 to this robust time-optimal control input are shown in Fig. 2.6 for four different values of $k = k_1 = k_2$. We notice that the resulting responses are less sensitive to parameter variations, as compared to the

responses to the ideal, time-optimal control input, as shown in Fig. 2.3. The second flexible mode is significantly excited during maneuvers, however. Performance robustness has been increased at the expense of the increased maneuvering time of 10.18 sec, as compared to the ideal minimum-time of 6.511 sec. It is, however, emphasized that simply prolonging the maneuver time does not help to reduce residual structural vibrations caused by modeling uncertainty; a proper pulse sequence is necessary.

2.3.3 Case 2-2 with Two One-Sided Control Inputs

For Case 2-2, we can represent the control inputs as follows:

$$\begin{aligned} u_1 &= u_s(t) - u_s(t-\Delta_0) + u_s(t-t_2) \\ &- u_s(t-t_2-\Delta_2) + u_s(t-t_4) - u_s(t-t_4-\Delta_4) \\ u_2 &= -u_s(t-t_1) + u_s(t-t_1-\Delta_1) - u_s(t-t_3) \\ &+ u_s(t-t_3-\Delta_3) - u_s(t-t_5) + u_s(t-t_5-\Delta_5) \end{aligned}$$

where we have 11 unknowns to be determined, and t_j and Δ_j are defined as in Fig. 2.2.

The robust time-optimal solution can then be obtained by solving the constrained parameter optimization problem

$$min\ J = t_f = t_5 + \Delta_5 \tag{2.75}$$

subject to

$$\begin{aligned} &\Delta_0 - \Delta_1 + \Delta_2 - \Delta_3 + \Delta_4 - \Delta_5 = 0 \\ &6 + \sum_{j=0}^{5}(-1)^j[\Delta_j^2 + 2t_j\Delta_j^2] = 0 \\ &\sum_{j=0,2,4}[\cos(\omega_2 t_j) - \cos(\omega_2(t_j+\Delta_j))] = 0 \end{aligned}$$

$$\sum_{j=0,2,4} [\sin(\omega_2 t_j) - \sin(\omega_2(t_j + \Delta_j))] = 0$$

$$2 \sum_{j=1,3} [\cos(\omega_3 t_j) - \cos(\omega_3(t_j + \Delta_j))]$$

$$+ \sum_{j=0,2,4} [\cos(\omega_3 t_j) - \cos(\omega_3(t_j + \Delta_j))] = 0$$

$$2 \sum_{j=1,3} [\sin(\omega_3 t_j) - \sin(\omega_3(t_j + \Delta_j))]$$

$$+ \sum_{j=0,2,4} [\sin(\omega_3 t_j) - \sin(\omega_3(t_j + \Delta_j))] = 0$$

$$\sum_{j=0,2,4} [t_j \cos(\omega_2 t_j) - (t_j + \Delta_j) \cos(\omega_2(t_j + \Delta_j))] = 0$$

$$\sum_{j=0,2,4} [t_j \sin(\omega_2 t_j) - (t_j + \Delta_j) \sin(\omega_2(t_j + \Delta_j))] = 0$$

$$2 \sum_{j=1,3} [t_j \cos(\omega_3 t_j) - (t_j + \Delta_j) \cos(\omega_3(t_j + \Delta_j))]$$

$$+ \sum_{j=0,2,4} [t_j \cos(\omega_3 t_j) - (t_j + \Delta_j) \cos(\omega_3(t_j + \Delta_j))] = 0$$

$$2 \sum_{j=1,3} [t_j \sin(\omega_3 t_j) - (t_j + \Delta_j) \sin(\omega_3(t_j + \Delta_j))]$$

$$+ \sum_{j=0,2,4} [t_j \sin(\omega_3 t_j) - (t_j + \Delta_j) \sin(\omega_3(t_j + \Delta_j))] = 0$$

$$\Delta_j \geq 0; \quad j = 0, 1, 2, 3, 4, 5$$

$$t_1,\ t_2,\ t_3,\ t_4,\ t_5 > 0\ ;\ t_0 = 0$$

A solution to this problem is:

$$\begin{aligned} t_0 &= 0.0000, \quad \Delta_0 = 0.5814 \\ t_1 &= 1.9948, \quad \Delta_1 = 0.5657 \\ t_2 &= 2.8533, \quad \Delta_2 = 1.2202 \\ t_3 &= 4.3234, \quad \Delta_3 = 1.4425 \\ t_4 &= 6.3455, \quad \Delta_4 = 0.5814 \\ t_5 &= 6.9850, \quad \Delta_5 = 0.3747 \\ t_f &= 7.36 \end{aligned} \tag{2.76}$$

The time responses of x_3 to the robust time-optimal control inputs are shown in Fig. 2.7 for four different values of $k = k_1 = k_2$. Similar to Case 2-1 of the preceding section, the robustness has been increased at the expense of the increased maneuvering time of 7.36 sec, as compared to the ideal minimum-

time of 5.35 sec. The jet on-time is 4.765 sec. The second flexible mode is less excited, as compared to Case 2-1.

2.3.4 Case 2-3 with Two One-Sided Control Inputs

Assuming that each control input has two pulses as in Case 2-2, we can represent the control inputs as:

$$\begin{aligned} u_1 &= u_s(t) - u_s(t-\Delta_0) + u_s(t-t_2) - u_s(t-t_2-\Delta_2) \\ &+ u_s(t-t_4) - u_s(t-t_4-\Delta_4) \\ u_3 &= -u_s(t-t_1) + u_s(t-t_1-\Delta_1) - u_s(t-t_3) \\ &+ u_s(t-t_3-\Delta_3) - u_s(t-t_5) + u_s(t-t_5-\Delta_5) \end{aligned}$$

where we have 11 unknowns to be determined, and t_j and Δ_j are defined as in Fig. 2.2.

The robust time-optimal solution can then be obtained by solving the constrained parameter optimization problem

$$min\ J = t_5 + \Delta_5 \tag{2.77}$$

subject to

$$\begin{aligned} &\Delta_0 - \Delta_1 + \Delta_2 - \Delta_3 + \Delta_4 - \Delta_5 = 0 \\ &6 + \sum_{j=0}^{5}(-1)^j[\Delta_j^2 + 2t_j\Delta_j^2] = 0 \\ &\sum_{j=0}^{5}(-1)^j[\sin(\omega_2 t_j) - \sin(\omega_2(t_j+\Delta_j))] = 0 \\ &\sum_{j=0}^{5}(-1)^j[\cos(\omega_2 t_j) - \cos(\omega_2(t_j+\Delta_j))] = 0 \\ &\sum_{j=0}^{5}[(-1)^j\sin(\omega_3 t_j) - \sin(\omega_3(t_j+\Delta_j))] = 0 \end{aligned}$$

$$\sum_{j=0}^{5}[(-1)^j \cos(\omega_3 t_j) - \cos(\omega_3(t_j + \Delta_j))] = 0$$

$$\sum_{j=0}^{5}(-1)^j[t_j \cos\omega_2 t_j - (t_j + \Delta_j)\cos\omega_2(t_j + \Delta_j)] = 0$$

$$\sum_{j=0}^{5}(-1)^j[t_j \sin\omega_2 t_j - (t_j + \Delta_j)\sin\omega_2(t_j + \Delta_j)] = 0$$

$$\sum_{j=0}^{5}(-1)^j[t_j \cos\omega_3 t_j - (t_j + \Delta_j)\cos\omega_3(t_j + \Delta_j)] = 0$$

$$\sum_{j=0}^{5}(-1)^j[t_j \sin\omega_3 t_j - (t_j + \Delta_j)\sin\omega_3(t_j + \Delta_j)] = 0$$

$$\Delta_j \geq 0; \quad j = 0, 1, 2, 3, 4, 5$$

$$t_1,\ t_2,\ t_3,\ t_4,\ t_5 > 0;\ \ t_0 = 0$$

A solution to this problem is

$$\begin{aligned} t_0 &= 0.000, \quad \Delta_0 = 0.2189 \\ t_1 &= 3.774, \quad \Delta_1 = 0.2609 \\ t_2 &= 2.030, \quad \Delta_2 = 0.3594 \\ t_3 &= 5.778, \quad \Delta_3 = 0.3594 \\ t_4 &= 4.152, \quad \Delta_4 = 0.2609 \\ t_5 &= 7.968, \quad \Delta_5 = 0.2189 \\ t_f &= 8.187 \end{aligned} \tag{2.78}$$

The time responses of x_3 to the robust time-optimal control inputs are shown in Fig. 2.8 for four different values of $k = k_1 = k_2$. The robustness has been increased at the expense of the increased maneuvering time of 8.187 sec, as compared to the ideal minimum-time of 4.362 sec. However, the control on-time is only *1.678 seconds!* Because of the properly coordinated pulse sequences, the flexible modes are not significantly excited during maneuvers and the residual responses after the maneuvers are well desensitized.

Now consider the effects of the accuracy of the switching time of firing

of the pulses. The solution of Case 2-3 is now truncated to 2 decimal places :

$$\begin{array}{ll} t_0 = 0.00, & \Delta_0 = 0.21 \\ t_1 = 3.77, & \Delta_1 = 0.26 \\ t_2 = 2.03, & \Delta_2 = 0.35 \\ t_3 = 5.77, & \Delta_3 = 0.35 \\ t_4 = 4.15, & \Delta_4 = 0.26 \\ t_5 = 7.96, & \Delta_5 = 0.21 \\ t_f = 8.18 & \end{array} \tag{2.79}$$

The time responses of x_3 to the robust time-optimal control inputs are shown in Fig. 2.9 for four different values of $k = k_1 = k_2$. The residual vibrations have not increased and the response is robust to the switching time. Now consider truncating the solution to one decimal place, which may be too unrealistic in practice, as follows:

$$\begin{array}{ll} t_0 = 0.0, & \Delta_0 = 0.2 \\ t_1 = 3.7, & \Delta_1 = 0.2 \\ t_2 = 2.0, & \Delta_2 = 0.3 \\ t_3 = 5.7, & \Delta_3 = 0.3 \\ t_4 = 4.1, & \Delta_4 = 0.2 \\ t_5 = 7.9, & \Delta_5 = 0.2 \\ t_f = 8.1 & \end{array} \tag{2.80}$$

The time responses of x_3 to the robust time-optimal control inputs are shown in Fig. 2.10 for four different values of $k = k_1 = k_2$. Again the residual vibrations have not increased but the steady-state solution has an offset.

2.4 Summary

In this chapter, we have demonstrated that the proposed *robustification* or *desensitization* approach does generate *robust* time-optimal open-loop control inputs for an uncertain dynamical system. Furthermore, on the contrary to a common notion, the results of this chapter indicate that properly coordinated, on-off pulse sequences can achieve a fast maneuvering time with a minimum of structural vibrations during and/or after a maneuver, even in

the face of plant modeling uncertainty. The time-optimal responses have been desensitized at the expense of the increased maneuvering time. It is again emphasized that simply prolonging the maneuver time does not help to reduce residual structural vibrations caused by modeling uncertainty; a proper coordination of pulse sequences is necessary, as demonstrated in this chapter.

Table 1: Summary of the results

Time-Optimal Control		
	$J^* = t_f$(sec)	Jet On-Time
Case 2-1	6.511	6.511
Case 2-2	5.340	4.172
Case 2-3	4.362	2.234
Robust Time-Optimal Control		
	$J^* = t_f$(sec)	Jet On-Time
Case 2-1	10.18	10.18
Case 2-2	7.360	4.765
Case 2-3	8.187	1.678

The results of this chapter are summarized in Table 1. As can be noticed in this table, it is natural to select the actuator configuration of Case 2-3, since this case provides the "best" overall performance in the sense of minimizing the maneuvering time, fuel consumption (jet on-time), and structural mode excitation. For Case 2-1, the maneuvering time and the jet on-time are the same, which is clearly undesirable from the viewpoint of fuel consumption. To avoid such undesirable continuous jet firings during a maneuver, a robust fuel- and time-optimal control problem will be treated in the following chapter.

2.5 Conclusions

A time-optimal open-loop control problem of flexible spacecraft in the face of modeling uncertainty has been investigated. The primary study

objective was to explore the feasibility of computing open-loop, on-off pulse control logic for uncertain flexible spacecraft. The results indicate that the proposed approach significantly reduces the residual structural vibrations caused by modeling uncertainty. The results also indicate the importance of a proper jet placement for practical trade-offs among the maneuvering time, fuel consumption, and performance robustness.

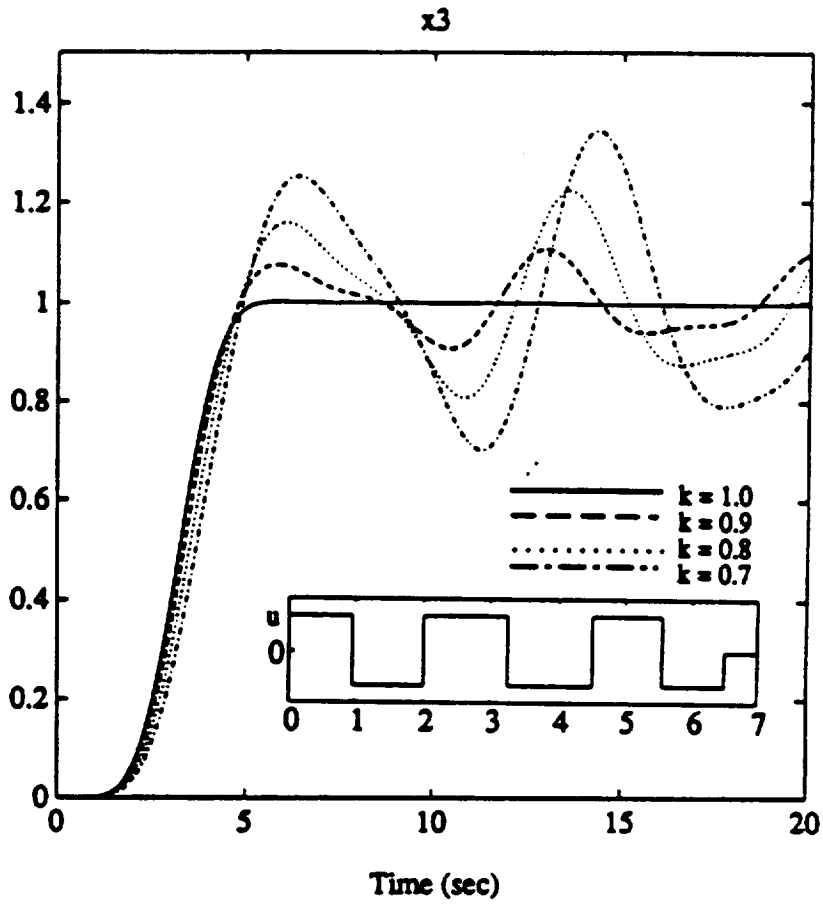

Figure 2.3: Responses of time-optimal control Case 2-1.

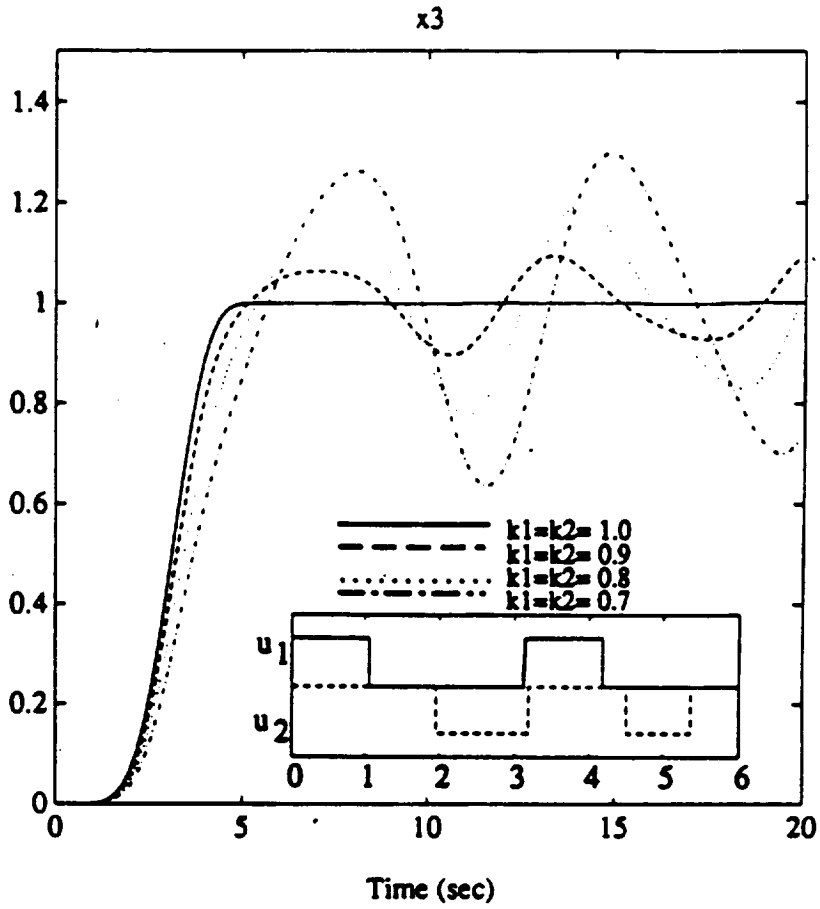

Figure 2.4: Responses of time-optimal control Case 2-2.

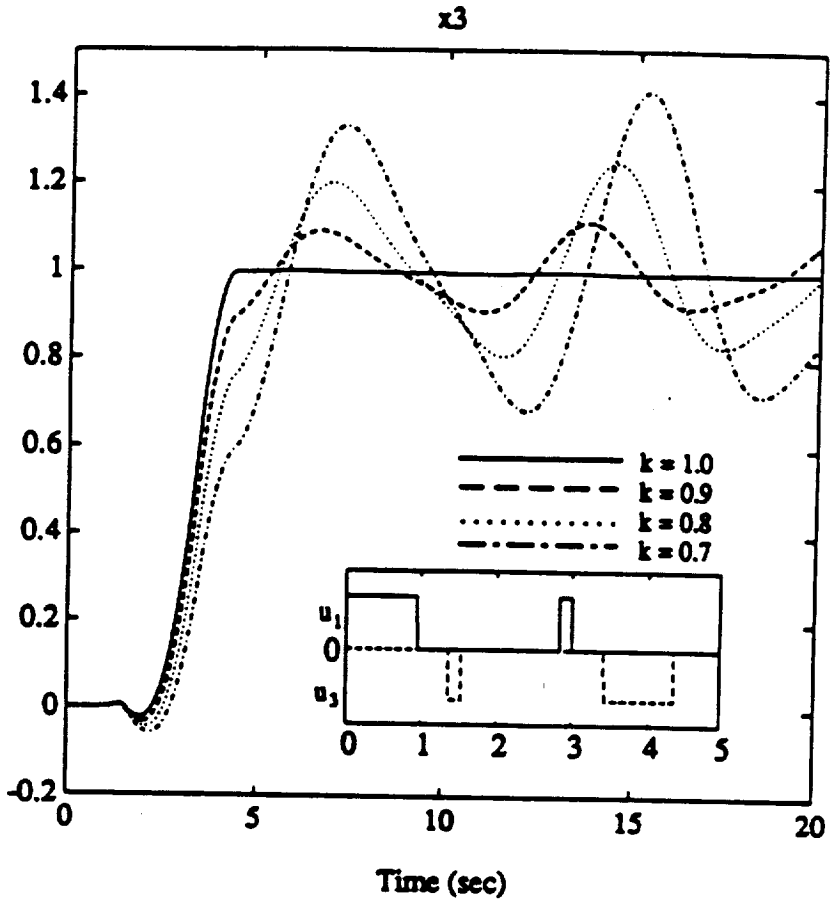

Figure 2.5: Responses of time-optimal control Case 2-3.

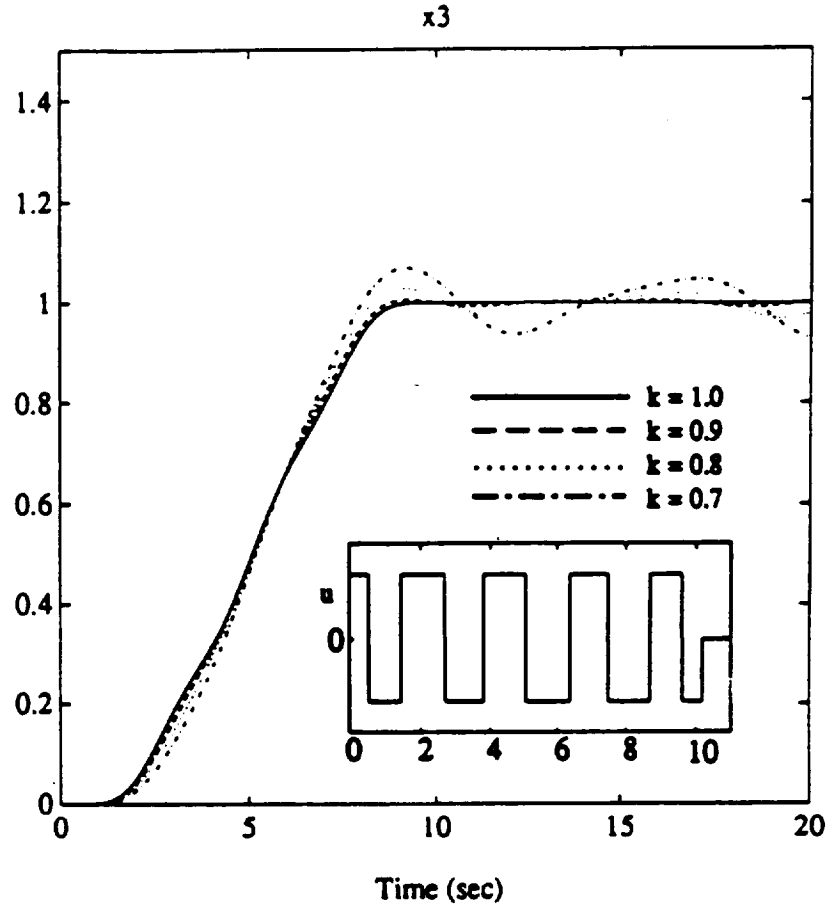

Figure 2.6: Responses of robust time-optimal control Case 2-1.

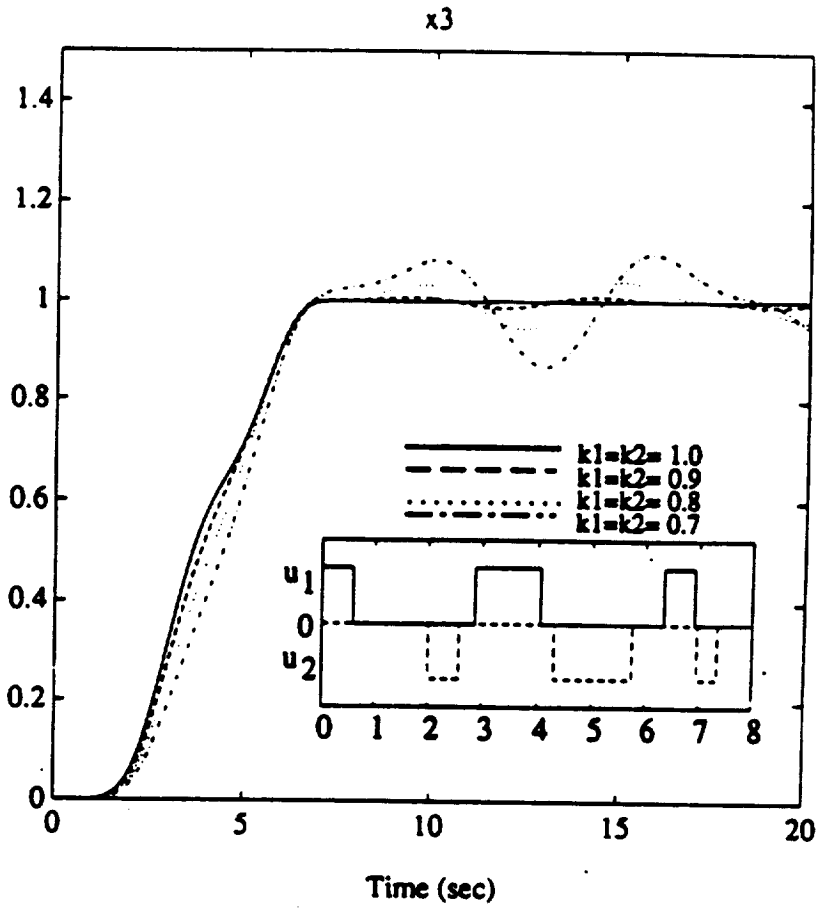

Figure 2.7: Responses of robust time-optimal control Case 2-2.

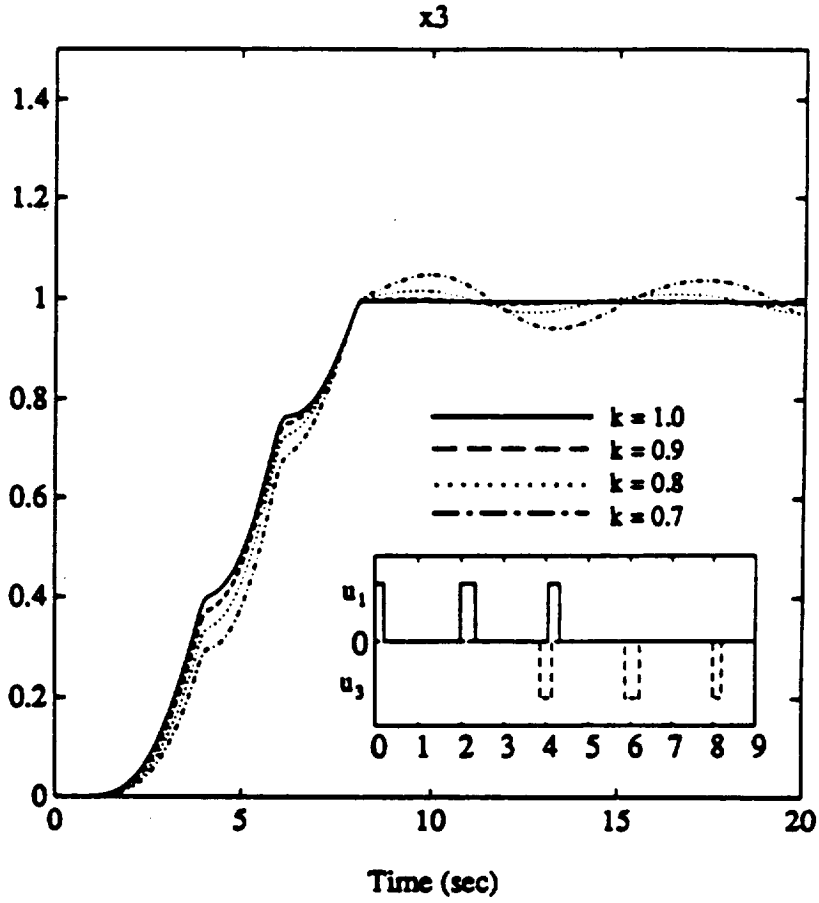

Figure 2.8: Responses of robust time-optimal control Case 2-3.

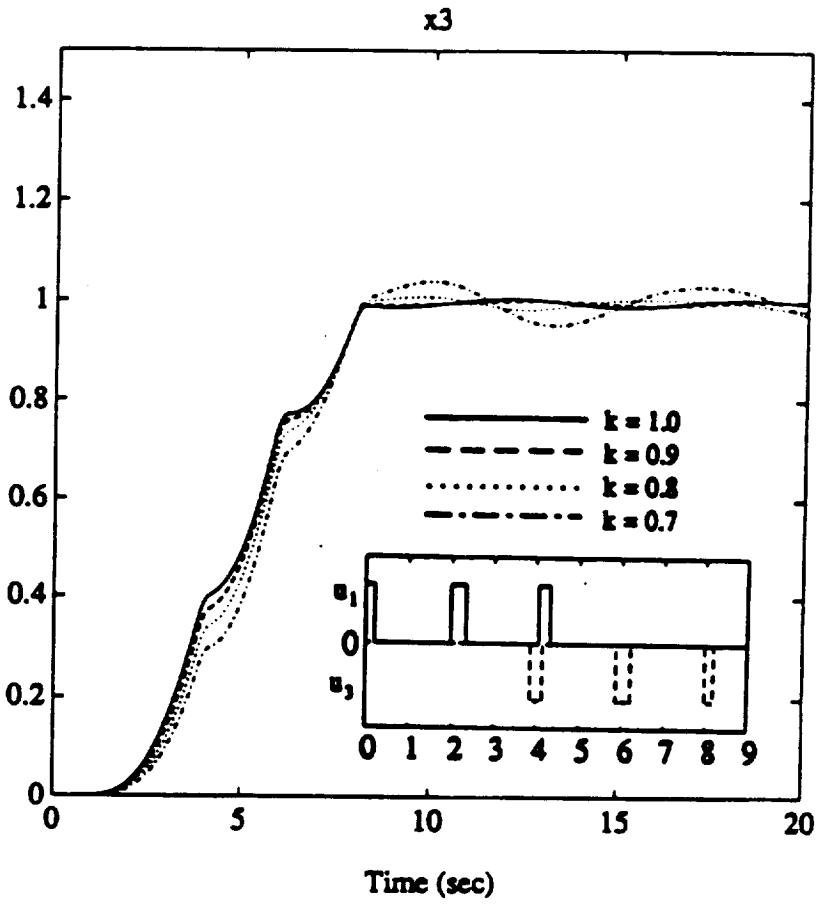

Figure 2.9: Responses of robust time-optimal control Case 2-3.

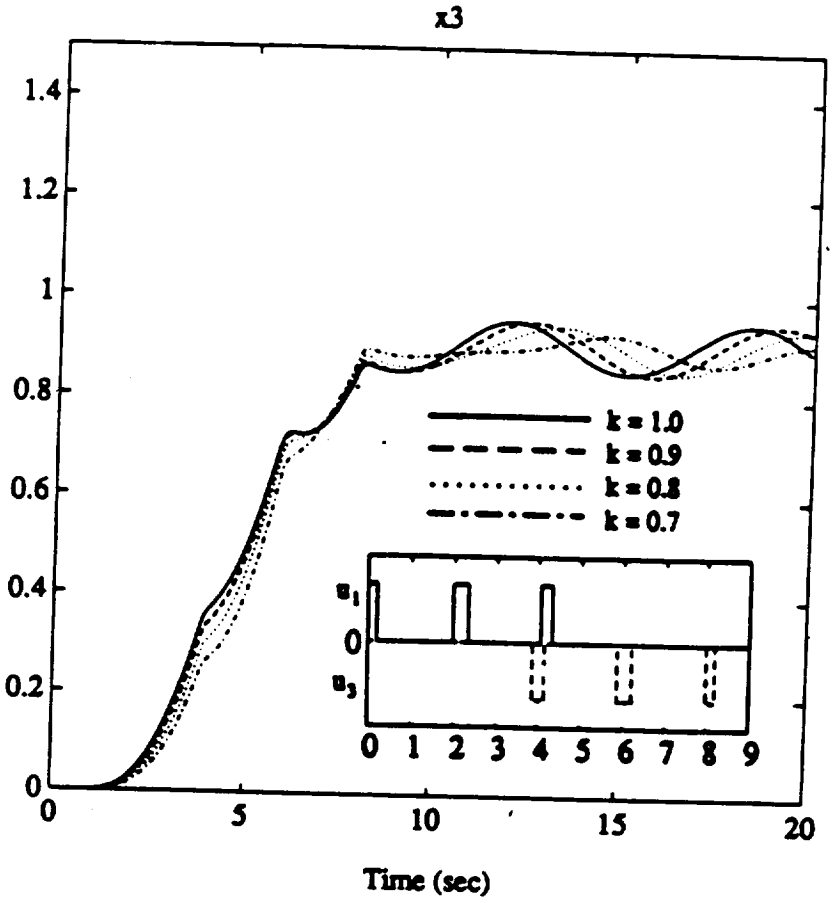

Figure 2.10: Responses of robust time-optimal control Case 2-3.

Chapter 3

Robust Fuel- and Time-Optimal Control of Uncertain Flexible Spacecraft

3.1 Introduction

The fuel- and time-optimal control problem of flexible spacecraft is in general a difficult problem to solve, even for a case without plant modeling uncertainty (e.g., see [14,15,16]). A standard, optimal control approach to such a problem requires an accurate plant model, and thus the resulting solution becomes sensitive to variations in model parameters. For this reason, a pulse-modulated, classical feedback controller is often employed for real spacecraft equipped with reaction jets [13,17].

In this chapter, however, we attempt to develop robustified, open-loop, fuel- and time-optimal control inputs for uncertain flexible spacecraft, which are often required to maneuver as quickly as possible without significant structural vibrations during and/or after a maneuver. In particular, we investigate the rest-to-rest maneuvering problem of a flexible spacecraft equipped with on-off reaction jets in the presence of uncertainty in model parameters. Expanding on the recent results of [11,12], we formulate a constrained optimization problem, where the objective function to be minimized is a weighted sum of the consumed fuel and the maneuvering time, with additional constraints for robustness with respect to plant modeling uncertainty.

We assume that the mass of the consumed fuel is small compared

with the mass of the spacecraft, and that the consumed fuel is proportional to the jet on-time. We further assume that the structural flexibility and mass distribution of the vehicle are more uncertain than the total mass of the system. Consequently, we focus on the robust control problem of flexible spacecraft in the face of modal frequency uncertainty. Furthermore, many theoretical and practical implementation issues inherent to a constrained parameter optimization problem are not elaborated in this chapter. The ultimate research goal of the future is to develop nonlinear feedback control logic for achieving the robust time-optimal performance similar to that presented in this chapter. As a first step toward such a research goal we emphasize the formulation of a robust fuel- and time-optimal control problem of flexible spacecraft and we investigate its solution in terms of switching patterns.

Other robustified, open-loop approaches attempt to find a smooth continuous forcing function (e.g., a versine function) that begins and ends with zero slope. The basic idea behind such approaches is that a smooth control input without sharp transitions is less likely to excite structural modes during maneuvers. The results of this chapter further confirm that most open-loop approaches, which utilize a smooth continuous control input so that structural modes are less likely to be excited, do not fully utilize the available control energy in performing a time-optimal maneuver.

The remainder of this chapter is organized as follows. Section 3.2 describes the fuel- and time-optimal control problem of flexible spacecraft without modeling uncertainty. The control problem is transformed into a parameter optimization problem in which the objective function is a sum of the final time and the jet on-time. A simple dynamical system with a rigid-mode and one/two flexible mode, shown in Fig. 3.1-3.3, is used to illustrate the concept. Three

cases (Case 3-1, Case 3-2 and Case 2-1) are explored (see Figs. 3.1-3.3). Section 3.3 describes the same problem that of Section 3.2 but with consideration of the presence of modeling uncertainty. Robustified fuel- and time-optimal solutions are then compared with an ideal solution obtained in Section 3.2.

3.2 Fuel- and Time-Optimal Control

3.2.1 Problem Formulation

Consider a flexible spacecraft described by

$$M\ddot{x} + Kx = Gu \tag{3.1}$$

where x is a generalized displacement vector, M a mass matrix, K a stiffness matrix, G the control input distribution matrix, and u the control input vector.

Equation (3.1) is transformed into the modal equation:

$$\ddot{y} + \Omega^2 y = \Phi u \tag{3.2}$$

where y is the modal coordinate vector, $\Omega^2 = diag(\omega_i^2)$, ω_i the i^{th} modal frequency ($\omega_1 = 0$ for the rigid body mode), and Φ the modal input distribution matrix.

In this chapter, we consider a simple model of a flexible spacecraft with a rigid-body mode and one dominant flexible mode, as shown in Fig. 3.1. We explore two cases for this system with two control inputs, u_+ and u_-, which are bounded as

$$0 \leq u_+ \leq +1 \tag{3.3}$$

$$-1 \leq u_- \leq 0 \tag{3.4}$$

For Case 3-1, both u_+ and u_- are acting on body 1, resulting in a typical case with a two-sided control input u_1 with $|u_1| \leq 1$. For Case 3-2, u_+ is placed

on body 1 and u_- is placed on body 2, resulting in a case with two one-sided control inputs: $u_1 = u_+$ and $u_2 = u_-$. For Case 2-1 both u_+ and u_- are acting on body 1, of the three mass-spring system.

The boundary conditions for the rest-to-rest maneuver are expressed in modal coordinates as:

$$\begin{array}{ll} y_1(0) = 0, & y_1(t_f) = 1 \\ \dot{y}_1(0) = 0, & \dot{y}_1(t_f) = 0 \\ y_i(0) = 0, & y_i(t_f) = 0 \\ \dot{y}_i(0) = 0, & \dot{y}_i(t_f) = 0 \end{array} \tag{3.5}$$

for $i = 2, ..., n$

For a fuel- and time-optimal control problem, the objective function to be minimized is, in general, a weighted sum of the maneuvering time and the consumed fuel. However, we consider here the following objective function which is simply a sum of the maneuvering time and the product of weight α and total jet on-time:

$$J = \int_0^{t_f} \{1 + \alpha(|u_+| + |u_-|)\} dt \tag{3.6}$$

The problem is then to find the control inputs which minimize the performance index J subject to Eqs.(3.2)-(3.4). In Section 3.3, we investigate the same problem as above but with additional robustness constraints with respect to plant modeling uncertainty.

3.2.2 Rigid Body Fuel- and Time Optimal Control

For a rigidized model of the nominal model discussed the equation of motion is

$$(m_1 + m_2)\ddot{x} = u \tag{3.7}$$

The rest-to-rest manuever, fuel- and time-optimal solution for the objective function given by Eq.(3.6) can be solved using control input as a combination of unit-step function u_s as

$$u = u_s(t) - u_s(t-\Delta) - u_s(t-t_1) + u_s(t-t_1-\Delta) \tag{3.8}$$

The solution is $\Delta = \sqrt{(m_1+m_2)/(2\alpha+1)}$ and $t_f = 2\Delta(\alpha+1) = 3.27$ sec for $\alpha = 1$. When this solution is applied to the flexible model there is residual vibration present and it remains even by prolonging maneuvering time for large weight α.

3.2.3 Parameter Optimization Problem

The control inputs u_+ and u_- can be expressed as a combination of unit-step function u_s as

$$u_+ = \sum_{j=0,2}^{N-1} [u_s(t-t_j) - u_s(t-t_j-\Delta_j)] \tag{3.9}$$

$$u_- = \sum_{j=1,3}^{N} [-u_s(t-t_j) + u_s(t-t_j-\Delta_j)] \tag{3.10}$$

which are in the form of one-sided pulse sequences as shown in Fig. 3.4. The j^{th} pulse starts at t_j and ends at $(t_j+\Delta_j)$. Δ_j is the j^{th} pulse duration. Due to the symmetric nature of the rest-to-rest maneuvering problem, we assume that u_+ and u_- have the same number of pulses, $(N+1)/2$, where N is defined as in Fig. 3.4.

Substituting Eq. (3.10) into Eq. (3.2) and incorporating the boundary conditions of Eq. (3.5), we get the time response of the rigid-body mode as

$$y_1(t \geq t_f) = \frac{1}{2}[\phi_{11} \sum_{j=0,2}^{N-1} (2t\Delta_j - 2t_j\Delta_j - \Delta_j^2) - \phi_{12} \sum_{j=1,3}^{N} (2t\Delta_j - 2t_j\Delta_j - \Delta_j^2)\ ] \tag{3.11}$$

where ϕ_{ij} is the (i,j) element of the modal input distribution matrix Φ. For a given boundary condition, $y_1(t \geq t_f) = 1$, the following constraint must hold

$$\phi_{11} \sum_{j=0,2}^{N-1} \Delta_j - \phi_{12} \sum_{j=1,3}^{N} \Delta_j = 0 \tag{3.12}$$

The rest-to-rest constraint for the rigid-body mode then becomes

$$2 - \phi_{11} \sum_{j=0,2}^{N-1} [2t_j\Delta_j - \Delta_j^2] + \phi_{12} \sum_{j=1,3}^{N} [2t_j\Delta_j - \Delta_j^2] = 0 \tag{3.13}$$

Substituting Eq. (3.10) into Eq. (3.2) and solving for the time response of the i^{th} flexible mode, we get

$$\begin{aligned} y_i(t) \quad &= \frac{1}{\omega_i^2} \cos(\omega_i t)[-\phi_{i1} \sum_{j=0,2}^{N-1} c_{ij} + \phi_{i2} \sum_{j=1,3}^{N} c_{ij}] \\ &+ \frac{1}{\omega_i^2} \sin(\omega_i t)[\phi_{i1} \sum_{j=0,2}^{N-1} s_{ij} - \phi_{i2} \sum_{j=1,3}^{N} s_{ij}] \end{aligned} \tag{3.14}$$

where

$$\begin{aligned} c_{ij} \quad &= \cos(\omega_i t_j) - \cos(\omega_i(t_j + \Delta_j)) \\ s_{ij} \quad &= \sin(\omega_i t_j) - \sin(\omega_i(t_j + \Delta_j)) \end{aligned}$$

for $t \geq t_f$.

Also, rest-to-rest maneuvering requires $y_i(t) = 0$ for $t \geq t_f$; i.e., we have the following flexible mode constraints for no residual structural vibration:

$$-\phi_{i1} \sum_{j=0,2}^{N-1} c_{ij} + \phi_{i2} \sum_{j=1,3}^{N} c_{ij} = 0 \tag{3.15}$$

$$\phi_{i1} \sum_{j=0,2}^{N-1} s_{ij} - \phi_{i2} \sum_{j=1,3}^{N} s_{ij} = 0 \tag{3.16}$$

for each flexible mode.

Since Eqs. (3.12), (3.13), and (2.14) are the necessary conditions for optimal solution, the fuel- and time-optimal control problem can be formulated as a constrained parameter optimization problem as follows:

$$min\ J \ = \ t_f + \alpha \sum_{j=0,1,2}^{N} \Delta_j \tag{3.17}$$

subject to the constraints given by Eqs. (3.12), (3.13) and (3.16).

3.2.4 Case 3-1

Consider a case where two control inputs u_+ and u_- both are acting on body 1. The control inputs are then assumed as:

$$u_+ \ = \ u_s(t) - u_s(t-\Delta) \tag{3.18}$$

$$u_- \ = \ -u_s(t-t_1) + u_s(t-t_1-\Delta) \tag{3.19}$$

where the pulse sequence is defined as shown in Fig. 3.2, and the maneuver time $t_f = t_1 + \Delta$. The nominal parameters are: $m_1 = m_2 = k = 1$ with appropriate units. The corresponding matrices Ω^2 and Φ in Eq. (3.2) are

$$\Omega^2 = \begin{bmatrix} 0 & 0 \\ 0 & 2 \end{bmatrix} \qquad \Phi = \frac{1}{2}\begin{bmatrix} 1 & 1 \\ 1 & 1 \end{bmatrix}$$

The constraint equations can be obtained as :

$$t_f\Delta - \Delta^2 - 2 = 0 \tag{3.20}$$

$$\cos(\omega t_f/2) - \cos(\omega(t_f/2 - \Delta)) = 0 \tag{3.21}$$

where $\omega = \sqrt{2}$.

The fuel- and time-optimal solution is obtained by solving the constrained minimization problem:

$$min\ J \ = \ t_f + 2\Delta$$

subject to the preceding constraints. The solution of this problem is obtained as

$$\begin{aligned} \Delta &= 0.45016 \\ t_1 &= 4.44288 \\ t_f &= 4.89304 \end{aligned} \tag{3.22}$$

The time responses of x_2 (the position of body 2) to the fuel- and time-optimal control inputs are shown in Fig. 3.5 for four different values of spring stiffness k. For the nominal case with $k = 1$, the jet on-time is now significantly reduced by 79% while the maneuvering time is increased by 18%, comparing to the time-optimal case. (The time-optimal solution for Case 2-1 of chapter 2 has both maneuvering time and control on-time of 4.128 sec.) As expected, however, significant residual structural vibrations can be seen in Fig. 3.5 due to variations in the uncertain parameter k.

3.2.5 Case 3-1b

Consider a special case of identical to Case 3-1 but with a longer maneuver time by increasing the weight α on the fuel in the cost function.

$$min\ J = t_f + 2\alpha\Delta$$

subject to the constraints given by Eqs(3.21). The solution of this problem for $\alpha = 10$ is obtained as

$$\begin{aligned} \Delta &= 0.225 \\ t_1 &= 8.88 \\ t_f &= 9.11 \end{aligned} \tag{3.23}$$

The time responses of x_2 (the position of body 2) to the fuel- and time-optimal control inputs are shown in Fig. 3.6 for four different values of spring stiffness k. The residual vibrations are still significant and are not reduced by increasing the maneuver time. Robustness to parameter variations is not achieved by increasing maneuver time.

3.2.6 Case 3-2

Consider Case 3-2 shown in Fig. 3.2 with two control inputs u_1 and u_2 acting on body 1 and body 2, respectively. The control inputs are assumed as

$$u_1 = u_s(t) - u_s(t-\Delta) \tag{3.24}$$

$$u_2 = -u_s(t-t_1) + u_s(t-t_1-\Delta) \tag{3.25}$$

and the maneuver time $t_f = t_1 + \Delta$. The matrices Ω^2 and Φ are

$$\Omega^2 = \begin{bmatrix} 0 & 0 \\ 0 & 2 \end{bmatrix} \qquad \Phi = \frac{1}{2}\begin{bmatrix} 1 & 1 \\ 1 & -1 \end{bmatrix}$$

The constraint equations can be obtained as :

$$t_f - 2/\Delta - \Delta = 0 \tag{3.26}$$

$$\sin(\omega t_f/2) + \sin(\omega(\Delta - t_f/2)) = 0 \tag{3.27}$$

The fuel- and time-optimal solution is obtained by solving the constrained minimization problem:

$$min\ J = t_f + 2\Delta$$

subject to the preceding constraints.

The solution is obtained as

$$\begin{aligned} \Delta &= 0.9003 \\ t_1 &= 2.2215 \\ t_f &= 3.1218 \end{aligned}$$

The time responses of x_2 to the fuel- and time-optimal control inputs are shown in Fig. 3.7 for four different values of spring stiffness k. Comparing to the time optimal case, the jet on-time is now significantly reduced by 56% while the maneuvering time is also reduced by 24%. This result indicates the importance of proper jet placement in the fuel- and time-optimal problem. As expected, significant residual structural vibrations can be seen in Fig. 3.7 due to variations in the uncertain parameter k.

3.2.7 Case 2-1

For Case 2-1, as illustrated in Fig. 3.3, two one-sided control inputs are bounded as

$$0 \leq u_+ \leq +1 \tag{3.28}$$

$$-1 \leq u_- \leq 0 \tag{3.29}$$

For this case, the time-optimal control inputs are assumed as:

$$\begin{aligned} u_1 &= u_s(t) - u_s(t - \Delta_0) \\ &+ u_s(t - t_2) - u_s(t - t_2 - \Delta_2) \end{aligned} \tag{3.30}$$

$$\begin{aligned} u_2 &= -u_s(t - t_1) + u_s(t - t_1 - \Delta_1) \\ &- u_s(t - t_3) + u_s(t - t_3 - \Delta_3) \end{aligned} \tag{3.31}$$

The modal equations for this case are

$$\ddot{y}_1 = 0.3333(u_+ + u_-) \tag{3.32}$$

$$\ddot{y}_2 + \omega_2^2 y_2 = 0.5(u_+ + u_-) \tag{3.33}$$

$$\ddot{y}_3 + \omega_3^2 y_3 = 0.1667(u_+ + u_-) \tag{3.34}$$

where $\omega_2 = 1$ and $\omega_3 = \sqrt{3}$. The rest-to-rest maneuver constraints are

$$\Delta_0 - \Delta_1 + \Delta_2 - \Delta_3 = 0 \tag{3.35}$$

$$6 + \sum_{j=0}^{3}(-1)^j[\Delta_j^2 - 2t_j\Delta_j] = 0 \tag{3.36}$$

$$\sum_{j=0}^{3}(-1)^j[\cos(\omega_2 t_j) - \cos(\omega_2(t_j + \Delta_j))] = 0 \tag{3.37}$$

$$\sum_{j=0}^{3}(-1)^j[\sin(\omega_2 t_j) - \sin(\omega_2(t_j + \Delta_j))] = 0 \tag{3.38}$$

$$\sum_{j=0}^{3}(-1)^j[\cos(\omega_3 t_j) - \cos(\omega_3(t_j + \Delta_j))] = 0 \tag{3.39}$$

$$\sum_{j=0}^{3}(-1)^j[\sin(\omega_3 t_j) - \sin(\omega_3(t_j + \Delta_j))] = 0 \tag{3.40}$$

The time-optimal solution can then be obtained by solving the constrained minimization problem:

$$min\ J = t_f + \sum_{i=0}^{3}\Delta_i \tag{3.41}$$

subject to the constraint given by Eqs. (3.40).

A solution of this problem can be found as

$$\begin{array}{ll} t_0 = 0.0000, & \Delta_0 = 0.400 \\ t_1 = 4.536, & \Delta_1 = 0.135 \\ t_2 = 2.582, & \Delta_2 = 0.135 \\ t_3 = 6.854, & \Delta_3 = 0.400 \\ t_f = 7.251 & \end{array} \tag{3.42}$$

The time responses of x_3 to the fuel and time-optimal control inputs are shown in Fig. 3.8 for four different values of $k = k_1 = k_2$. Now consider the time

response of the rigid body fuel- and time-optimal control solutions with final time $t_f = 7.35$ seconds. The residual vibrations are much larger and the flexible mode is significantly excited as shown in Fig. 3.9.(Rigidized Case 2-1)

3.2.8 Case 2-1b

Consider a special case of identical to Case 2-1 but with a longer maneuver time by increasing the weight α on the fuel in the cost function.

$$min\ J = t_f + \alpha \sum_{i=0}^{3} \Delta_i \tag{3.43}$$

subject to the constraint given by Eqs. (3.40).

A solution of this problem for $\alpha = 14$ can be found as

$$\begin{array}{ll} t_0 = 0.0000, & \Delta_0 = 0.153 \\ t_1 = 11.762, & \Delta_1 = 0.092 \\ t_2 = 2.152, & \Delta_2 = 0.092 \\ t_3 = 13.854, & \Delta_3 = 0.153 \\ t_f = 14 & \end{array} \tag{3.44}$$

The time responses of x_3 to the fuel and time-optimal control inputs are shown in Fig. 3.10 for four different values of $k = k_1 = k_2$. The residual vibrations are still significant and are not reduced by increasing the maneuver time. Robustness to parameter variations is not achieved by increasing maneuver time.

3.3 Robust Fuel- and Time-Optimal Control

3.3.1 Problem Formulation

As illustrated in Figs. 3.5 and 3.7, a standard, optimal control approach requires an accurate plant model and thus the resulting solution is not robust to plant modeling uncertainty. For this reason, an open-loop optimal control approach is seldom used in practice. In this section, we attempt to

develop robust, open-loop, fuel- and time-optimal control inputs for flexible spacecraft. Expanding on the results of the previous section, we formulate a parameter optimization problem, where the objective function to be minimized is a weighted sum of the consumed fuel and the maneuvering time, with additional constraints for robustness with respect to structural frequency uncertainty.

To attenuate residual vibrations of the flexible modes, the energy of the residual vibrations should be minimized, where the energy of the residual vibration is proportional to the square of the amplitude. Thus, Eq. (3.14) can be written as

$$y_i(t \geq t_f) = A\sin(\omega_i t) + B\cos(\omega_i t) \tag{3.45}$$

where A, B are functions of ω_i and ϕ_{ij} and

$$C^2 = A^2 + B^2 \tag{3.46}$$

$$\frac{dC^2}{dp_i} = \frac{dC^2}{d\omega_k}\frac{d\omega_k}{dp_i} \tag{3.47}$$

where p_i is the i^{th} uncertain parameter. For these derivatives to be zero ($t \geq t_f$), we get

$$-\phi_{i1}\sum_{j=0,2}^{N-1} g_{ij} + \phi_{i2}\sum_{j=1,3}^{N} g_{ij} = 0 \tag{3.48}$$

$$\phi_{i1}\sum_{j=0,2}^{N-1} h_{ij} - \phi_{i2}\sum_{j=1,3}^{N} h_{ij} = 0 \tag{3.49}$$

where

$$g_{ij} = t_j\cos(\omega_i t_j) - (t_j + \Delta_j)\cos(\omega_i(t_j + \Delta_j)) \tag{3.50}$$

$$h_{ij} = t_j\sin(\omega_i t_j) - (t_j + \Delta_j)\sin(\omega_i(t_j + \Delta_j)) \tag{3.51}$$

Eqs. (3.48)-(3.49) are called the first-order robustness constraints. Similarly, the r^{th}order robustness constraints can be expressed as

$$\begin{aligned} g_{ij} &= (t_j)^m \cos(\omega_i t_j) \\ &\quad -(t_j + \Delta_j)^m \cos(\omega_i (t_j + \Delta_j)) \end{aligned} \tag{3.52}$$

$$\begin{aligned} h_{ij} &= (t_j)^m \sin(\omega_i t_j) \\ &\quad -(t_j + \Delta_j)^m \sin(\omega_i (t_j + \Delta_j)) \end{aligned} \tag{3.53}$$

for $m = 1, 2, \cdots, r$.

These robustness constraints are incorporated in the constrainted parameter optimization problem formulation. Consequently, the number of pulses for each control input is changed to match the increased number of constraints. As an example, we consider the first-order robustness constraint, incorporated with the rest-to-rest maneuver constraints, to determine robust fuel- and time-optimal pulse sequences.

3.3.2 Case 3-1

Assuming that each input has two pulses, we can represent the control inputs as follows:

$$\begin{aligned} u_+ &= u_s(t) - u_s(t - \Delta_0) + u_s(t - t_2) \\ &\quad -u_s(t - t_2 - \Delta_2) \end{aligned} \tag{3.54}$$

$$\begin{aligned} u_- &= -u_s(t - t_1) + u_s(t - t_1 - \Delta_1) - u_s(t - t_3) \\ &\quad +u_s(t - t_3 - \Delta_3) \end{aligned} \tag{3.55}$$

where there are 7 unknowns to be determined, and t_j and Δ_j are defined as shown in Fig. 3.3.

The robust fuel- and time-optimal solution can then be obtained by solving the constrained parameter optimization problem:

$$min\ J = t_3 + \Delta_3 + (\Delta_0 + \Delta_1 + \Delta_2 + \Delta_3) \tag{3.56}$$

subject to

$$\Delta_0 - \Delta_1 + \Delta_2 - \Delta_3 = 0$$

$$\sum_{j=0}^{3}(-1)^j[2t_j\Delta_j + \Delta_j^2] + 4 = 0$$

$$\sum_{j=0}^{3}(-1)^j[\cos\omega t_j - \cos\omega(t_j + \Delta_j)] = 0$$

$$\sum_{j=0}^{3}(-1)^j[\sin\omega t_j - \sin\omega(t_j + \Delta_j)] = 0$$

$$\sum_{j=0}^{3}(-1)^j[t_j\cos\omega t_j - (t_j + \Delta_j)\cos\omega(t_j + \Delta_j)] = 0$$

$$\sum_{j=0}^{3}(-1)^j[t_j\sin\omega t_j - (t_j + \Delta_j)\sin\omega(t_j + \Delta_j)] = 0$$

$$\Delta_j \geq 0; \quad j = 0, 1, 2, 3$$

$$t_1,\ t_2,\ t_3 > 0$$

A solution to this problem is obtained as:

$$\begin{aligned} t_0 &= 0.0000, \quad \Delta_0 = 0.2379 \\ t_1 &= 4.1575, \quad \Delta_1 = 0.2489 \\ t_2 &= 2.3732, \quad \Delta_2 = 0.2489 \\ t_3 &= 6.5418, \quad \Delta_3 = 0.2379 \end{aligned} \tag{3.57}$$

The time responses of x_2 to this robust fuel- and time-optimal control inputs are shown in Fig. 3.11 for four different values of k. It can be seen that the robustness has been significantly increased at the expense of the increased maneuvering time of 6.78 sec. The jet on-time is 0.97 sec. Fig. 3.11 illustrates the reduction in residual vibration.

3.3.3 Case 3-2

Now consider Case 3-2 with two control inputs expressed as:

$$\begin{aligned} u_1 &= u_s(t) - u_s(t-\Delta_0) + u_s(t-t_2) \\ &\quad -u_s(t-t_2-\Delta_2) \end{aligned} \tag{3.58}$$

$$\begin{aligned} u_2 &= -u_s(t-t_1) + u_s(t-t_1-\Delta_1) - u_s(t-t_3) \\ &\quad +u_s(t-t_3-\Delta_3) \end{aligned} \tag{3.59}$$

where there are 7 unknowns to be determined.

The problem is to minimize the following objective function

$$min\ J = t_3 + \Delta_3 + (\Delta_0 + \Delta_1 + \Delta_2 + \Delta_3) \tag{3.60}$$

subject to

$$\Delta_0 - \Delta_1 + \Delta_2 - \Delta_3 = 0$$

$$\sum_{j=0}^{3}(-1)^j[2t_j\Delta_j + \Delta_j^2] + 4 = 0$$

$$\sum_{j=0}^{3}[\cos\omega t_j - \cos\omega(t_j+\Delta_j)] = 0$$

$$\sum_{j=0}^{3}[\sin\omega t_j - \sin\omega(t_j+\Delta_j)] = 0$$

$$\sum_{j=0}^{3}[t_j\cos\omega t_j - (t_j+\Delta_j)\cos\omega(t_j+\Delta_j)] = 0$$

$$\sum_{j=0}^{3}[t_j\sin\omega t_j - (t_j+\Delta_j)\sin\omega(t_j+\Delta_j)] = 0$$

$$\Delta_j \geq 0; \quad j = 0,1,2,3$$

$$t_1,\ t_2,\ t_3 > 0$$

A solution to this problem is obtained as:

$$\begin{array}{ll} t_0 = 0.0000, & \Delta_0 = 0.3762 \\ t_1 = 2.5918, & \Delta_1 = 0.4238 \\ t_2 = 1.9151, & \Delta_2 = 0.4238 \\ t_3 = 4.5545, & \Delta_3 = 0.3762 \end{array} \tag{3.61}$$

The time responses of x_2 to this robust fuel- and time-optimal control inputs are shown in Fig. 3.12 for four different values of k.

From Fig. 3.12, we notice that the residual vibration has been reduced considerably.

3.3.4 Case 2-1

For Case 2-1, we can represent the control inputs as follows:

$$\begin{aligned} u_+ &= u_s(t) - u_s(t-\Delta_0) + u_s(t-t_2) \\ &- u_s(t-t_2-\Delta_2) + u_s(t-t_4) - u_s(t-t_4-\Delta_4) \\ u_- &= -u_s(t-t_1) + u_s(t-t_1-\Delta_1) - u_s(t-t_3) \\ &+ u_s(t-t_3-\Delta_3) - u_s(t-t_5) + u_s(t-t_5-\Delta_5) \end{aligned}$$

where we have 11 unknowns to be determined, and t_j and Δ_j are defined as in Fig. 3.3.

The robust time-optimal solution can then be obtained by solving the constrained parameter optimization problem

$$min\ J = t_f + \sum_{i=0}^{5} \Delta_i \tag{3.62}$$

subject to

$$\Delta_0 - \Delta_1 + \Delta_2 - \Delta_3 + \Delta_4 - \Delta_5 = 0$$

$$6 + \sum_{j=0}^{5} (-1)^j [\Delta_j^2 - 2t_j\Delta_j] = 0$$

$$\sum_{j=0}^{5}(-1)^j[\cos(\omega_2 t_j) - \cos(\omega_2(t_j + \Delta_j))] = 0$$

$$\sum_{j=0}^{5}(-1)^j[\sin(\omega_2 t_j) - \sin(\omega_2(t_j + \Delta_j))] = 0$$

$$\sum_{j=0}^{5}(-1)^j[\cos(\omega_3 t_j) - \cos(\omega_3(t_j + \Delta_j))] = 0$$

$$\sum_{j=0}^{5}(-1)^j[\sin(\omega_3 t_j) - \sin(\omega_3(t_j + \Delta_j))] = 0$$

$$\sum_{j=0}^{5}(-1)^j[t_j\cos(\omega_2 t_j) - (t_j + \Delta_j)\cos(\omega_2(t_j + \Delta_j))] = 0 \ .$$

$$\sum_{j=0}^{5}(-1)^j[t_j\sin(\omega_2 t_j) - (t_j + \Delta_j)\sin(\omega_2(t_j + \Delta_j))] = 0$$

$$\sum_{j=0}^{5}(-1)^j[t_j\cos(\omega_3 t_j) - (t_j + \Delta_j)\cos(\omega_3(t_j + \Delta_j))] = 0$$

$$\sum_{j=0}^{5}(-1)^j[t_j\sin(\omega_3 t_j) - (t_j + \Delta_j)\sin(\omega_3(t_j + \Delta_j))] = 0$$

$$\Delta_j \geq 0; \quad j = 0,1,2,3,4,5$$

$$t_1,\ t_2,\ t_3,\ t_4,\ t_5 > 0\ ;\ t_0 = 0$$

A solution to this problem is:

$$\begin{aligned} t_0 &= 0.0000, \quad \Delta_0 = 0.1209 \\ t_1 &= 6.6158, \quad \Delta_1 = 0.1411 \\ t_2 &= 2.3022, \quad \Delta_2 = 0.2018 \\ t_3 &= 9.0502, \quad \Delta_3 = 0.2018 \\ t_4 &= 4.7973, \quad \Delta_4 = 0.1411 \\ t_5 &= 11.433, \quad \Delta_5 = 0.1209 \\ t_f &= 11.554 \end{aligned} \tag{3.63}$$

The time responses of x_3 to the robust fuel and time-optimal control inputs are shown in Fig. 3.13 for four different values of $k = k_1 = k_2$. The jet on-time is 0.927 sec. Now consider the time response of the rigid body fuel- and time-optimal control solutions with final time $t_f = 11.2$ seconds. The residual vibrations are much larger and the flexible mode is easily excited as shown in

Fig. 3.14. Thus the flexible modes cannot be neglected in the model for they can be easily excited.

Now consider the effects of uncertainty in the switching time of firing of the pulses. The solution of Case 2-1 is now truncated to 2 decimal places :

$$\begin{array}{ll} t_0 = 0.00, & \Delta_0 = 0.12 \\ t_1 = 6.61, & \Delta_1 = 0.14 \\ t_2 = 2.30, & \Delta_2 = 0.20 \\ t_3 = 9.05, & \Delta_3 = 0.20 \\ t_4 = 4.79, & \Delta_4 = 0.14 \\ t_5 = 11.4, & \Delta_5 = 0.12 \\ t_f = 11.5 & \end{array} \tag{3.64}$$

The time responses of x_3 to the robust time-optimal control inputs are shown in Fig. 3.15 for four different values of $k = k_1 = k_2$. The residual vibrations have not increased and the response is robust to the switching time. Now consider truncating the solution to one decimal place as:

$$\begin{array}{ll} t_0 = 0.0, & \Delta_0 = 0.1 \\ t_1 = 6.6, & \Delta_1 = 0.1 \\ t_2 = 2.3, & \Delta_2 = 0.2 \\ t_3 = 9.0, & \Delta_3 = 0.2 \\ t_4 = 4.7, & \Delta_4 = 0.1 \\ t_5 = 11.4, & \Delta_5 = 0.1 \\ t_f = 11.5 & \end{array} \tag{3.65}$$

The time responses of x_3 to the robust time-optimal control inputs are shown in Fig. 3.16 for four different values of $k = k_1 = k_2$. Again the residual vibrations have not increased but the overall rigid body motion has an offset.

3.4 Conclusions

Robust fuel- and time-optimal control problem of flexible spacecraft in the face of modeling uncertainty has been investigated. In particular, the rest-to-rest maneuvering problem of a flexible spacecraft equipped with on-off

reaction jets is considered. The rigid body solution is shown to have significant residual vibrations even for cases with prolonged maneuver time and it is necessary to include the flexible modes in the model. The results indicate that the proposed approach significantly reduces the residual structural vibrations caused by modeling uncertainty.

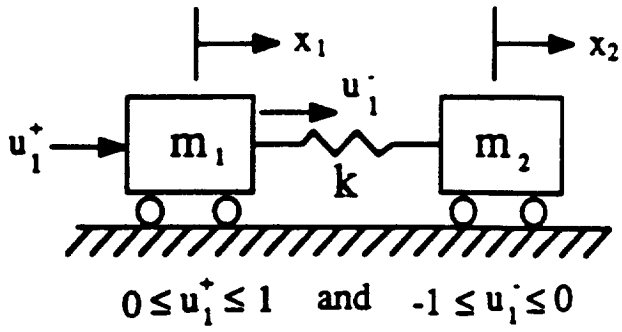

Figure 3.1: Case 3-1

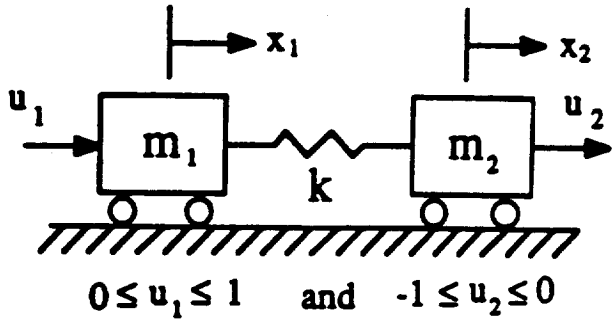

Figure 3.2: Case 3-2

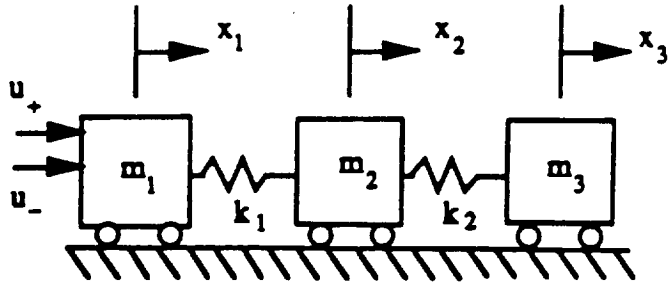

Figure 3.3: Case 2-1

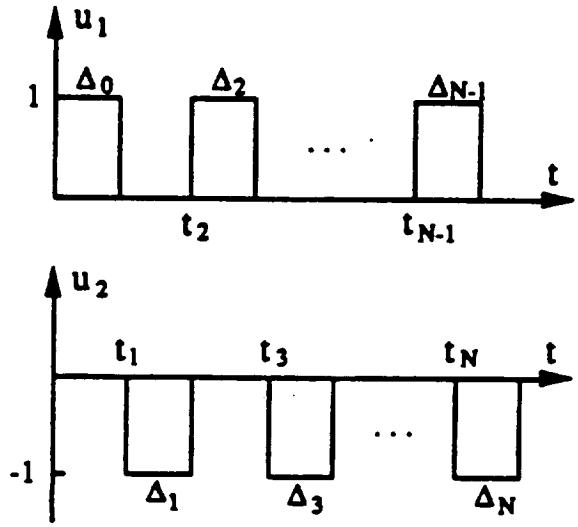

Figure 3.4: Pulse sequences.

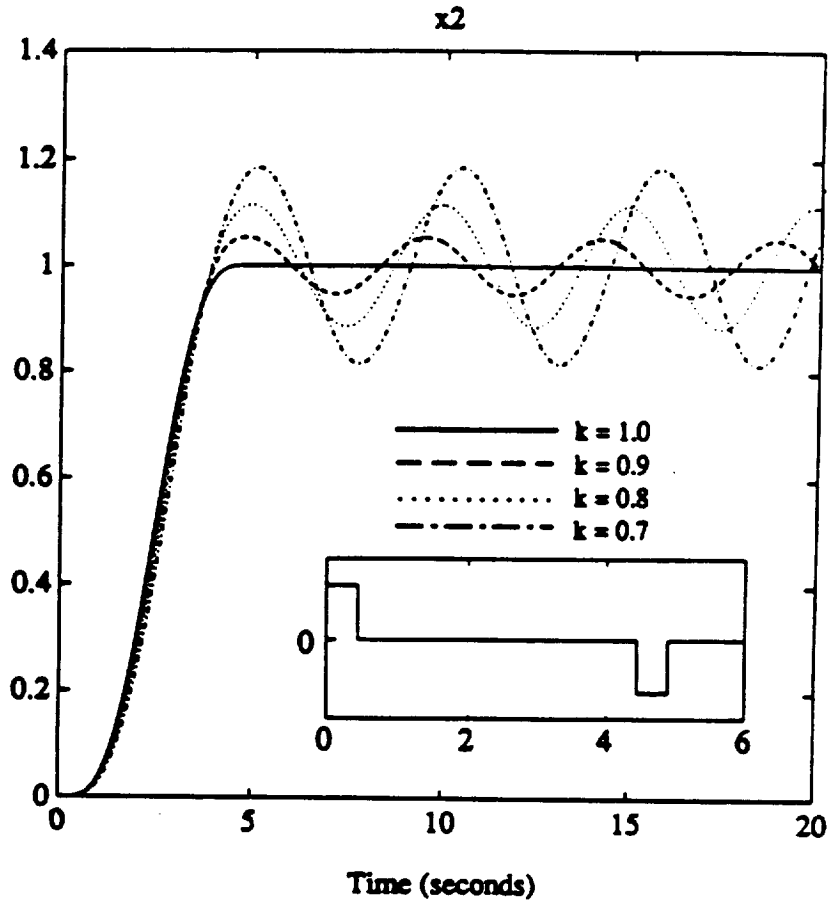

Figure 3.5: Responses to fuel and time-optimal control input (Case 3-1).

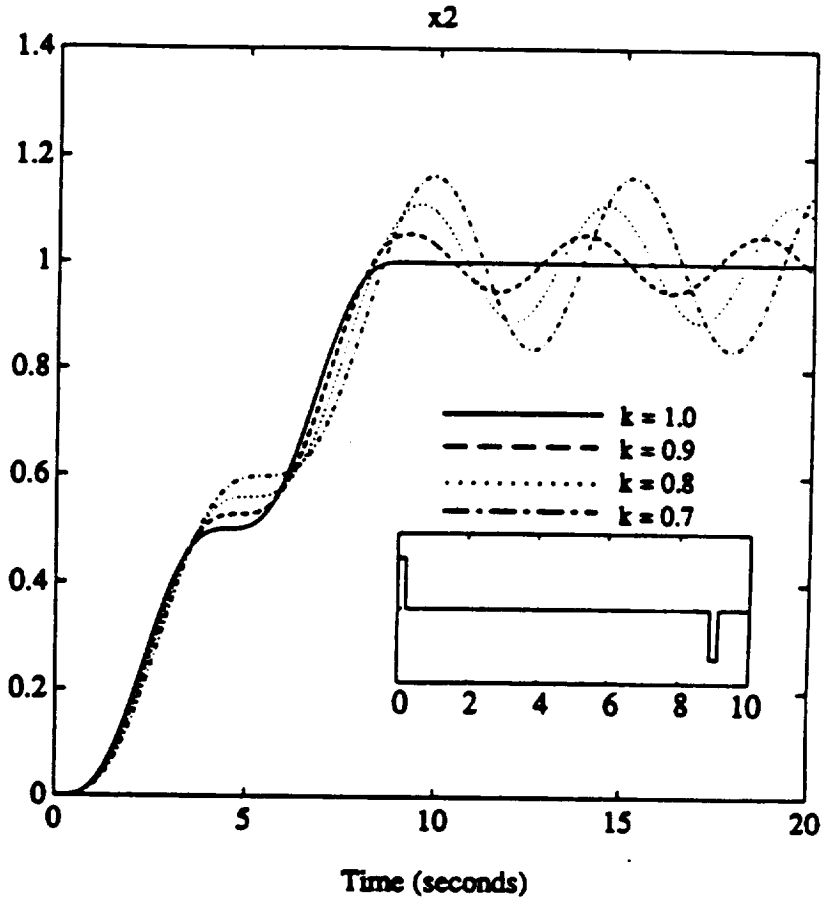

Figure 3.6: Responses to fuel and time-optimal control input (Case 3-1b).

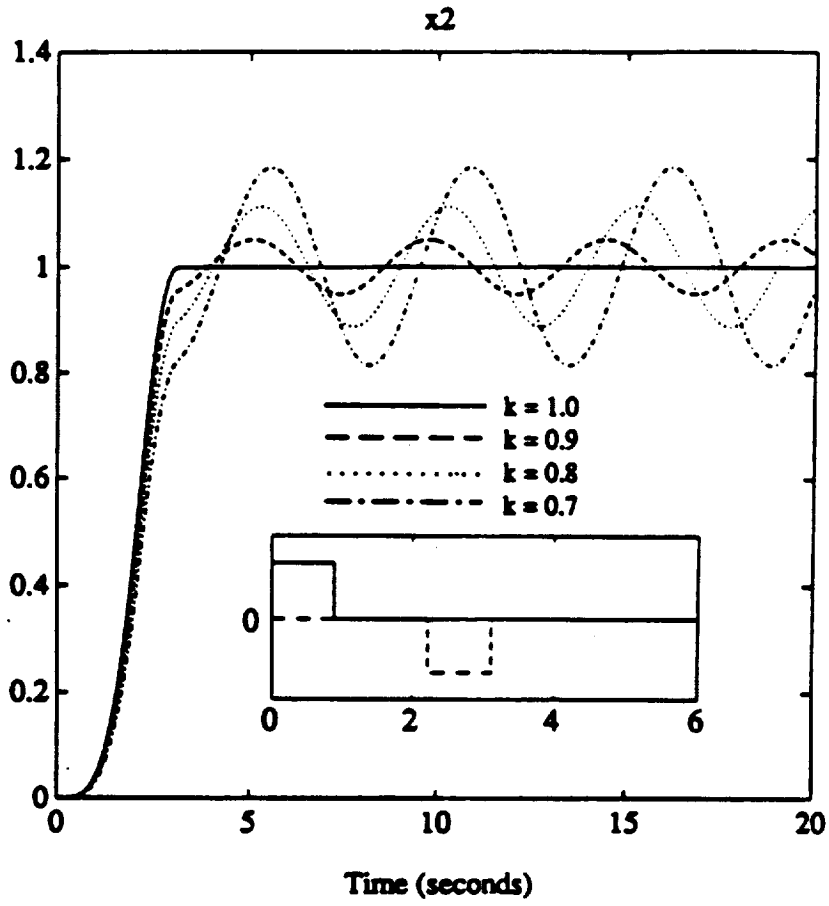

Figure 3.7: Responses to fuel and time-optimal control input (Case 3-2).

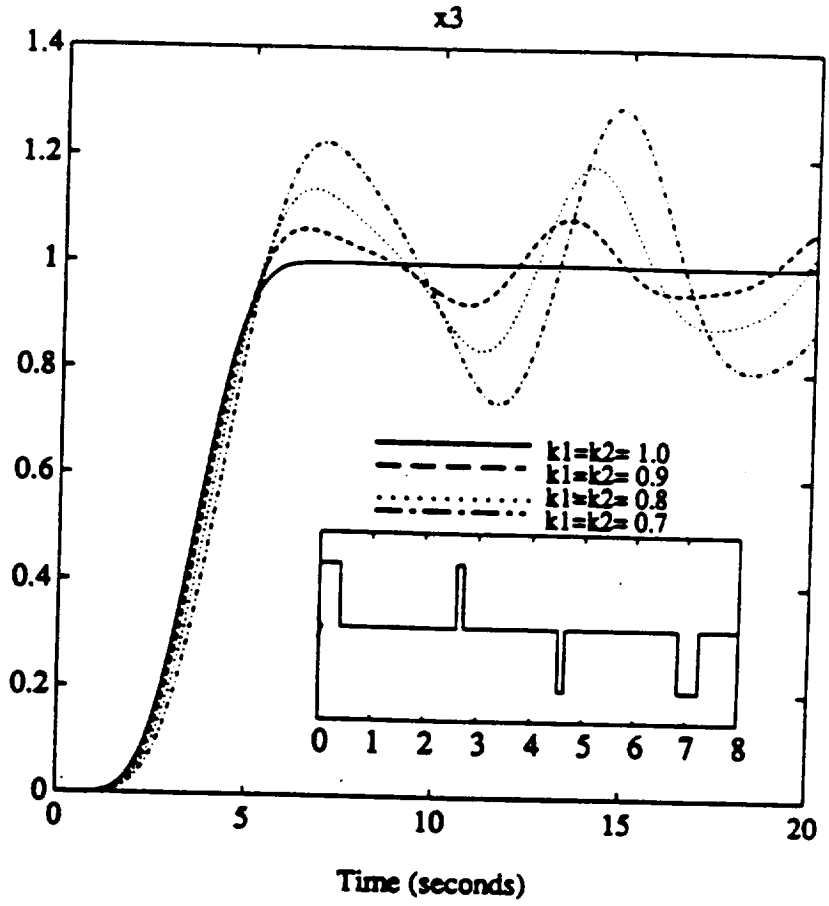

Figure 3.8: Responses to fuel and time-optimal control input (Case 2-1).

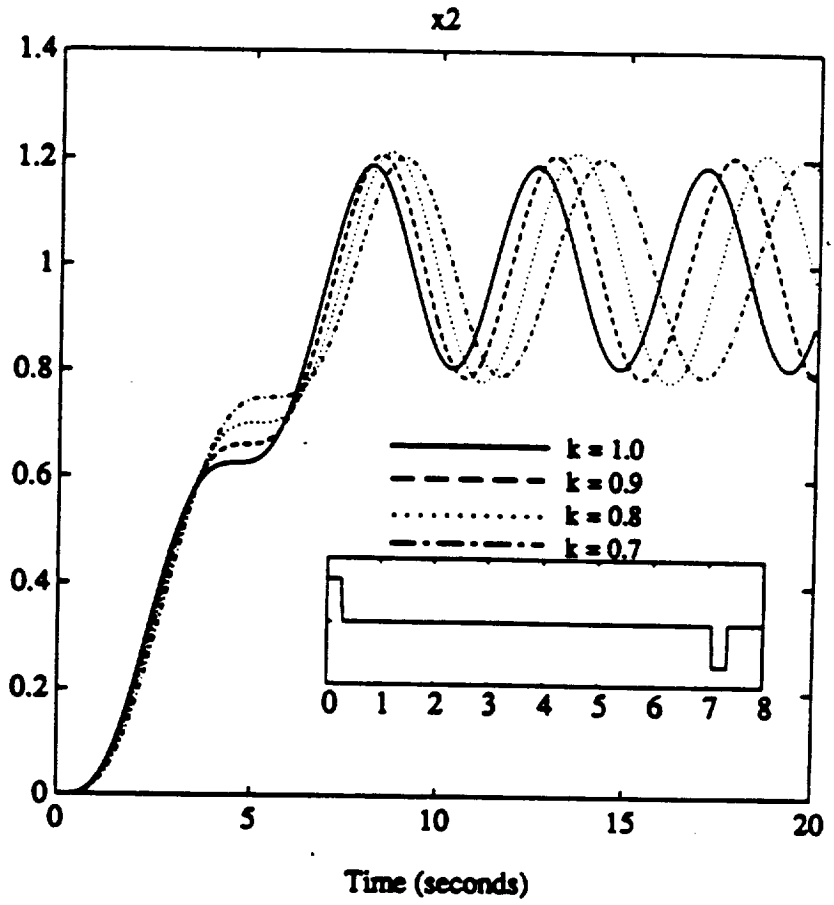

Figure 3.9: Responses to fuel and time-optimal control input (Rigid Body Solution).

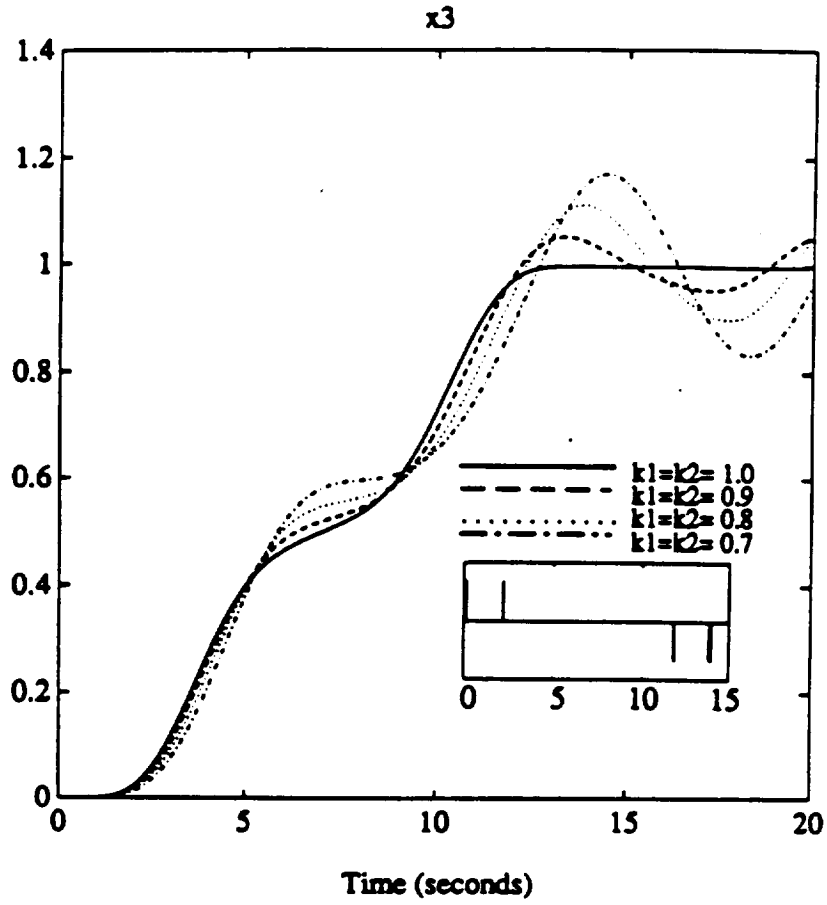

Figure 3.10: Responses to fuel and time-optimal control input (Case 2-1b).

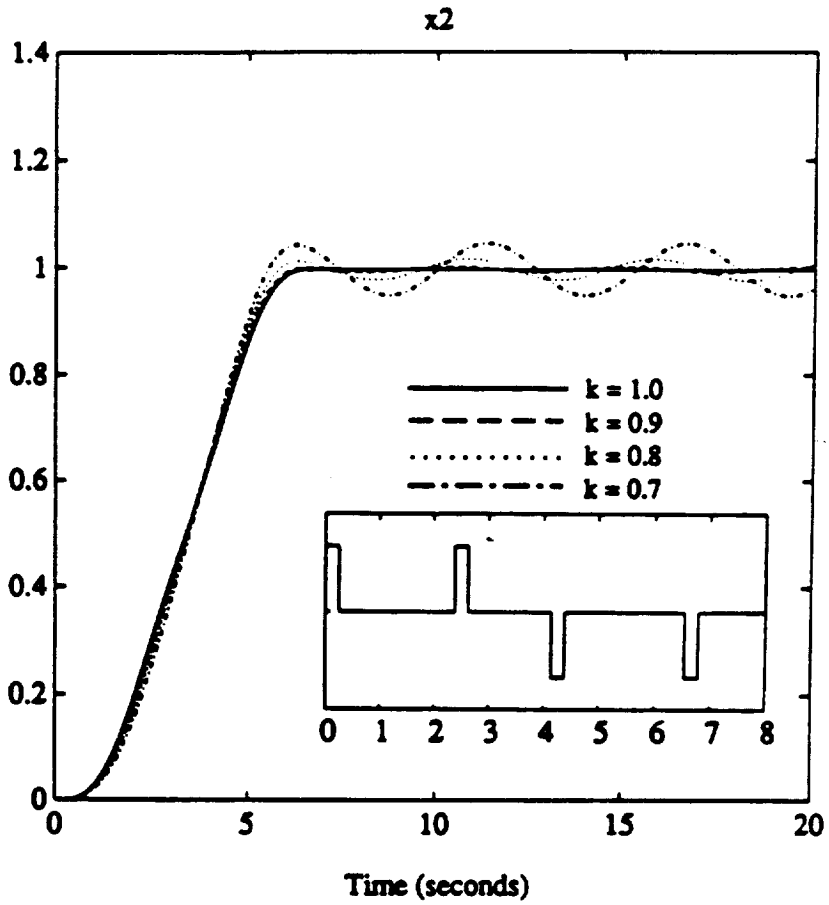

Figure 3.11: Responses to robust fuel and time-optimal control input (Case 3-1).

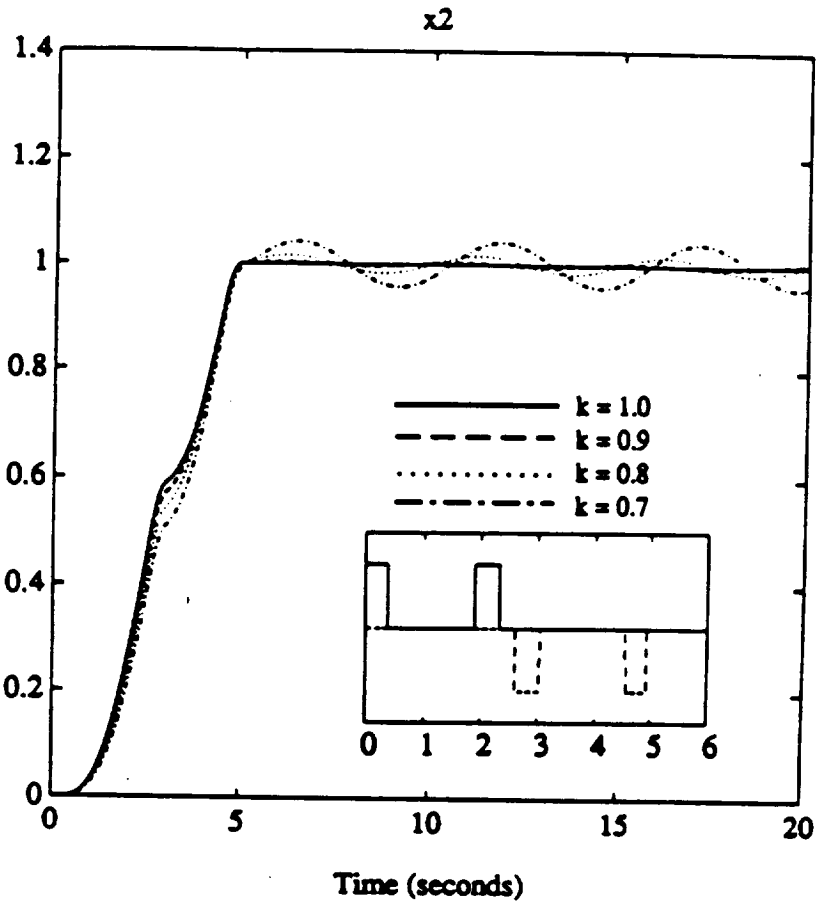

Figure 3.12: Responses to robust fuel and time-optimal control input (Case 3-2).

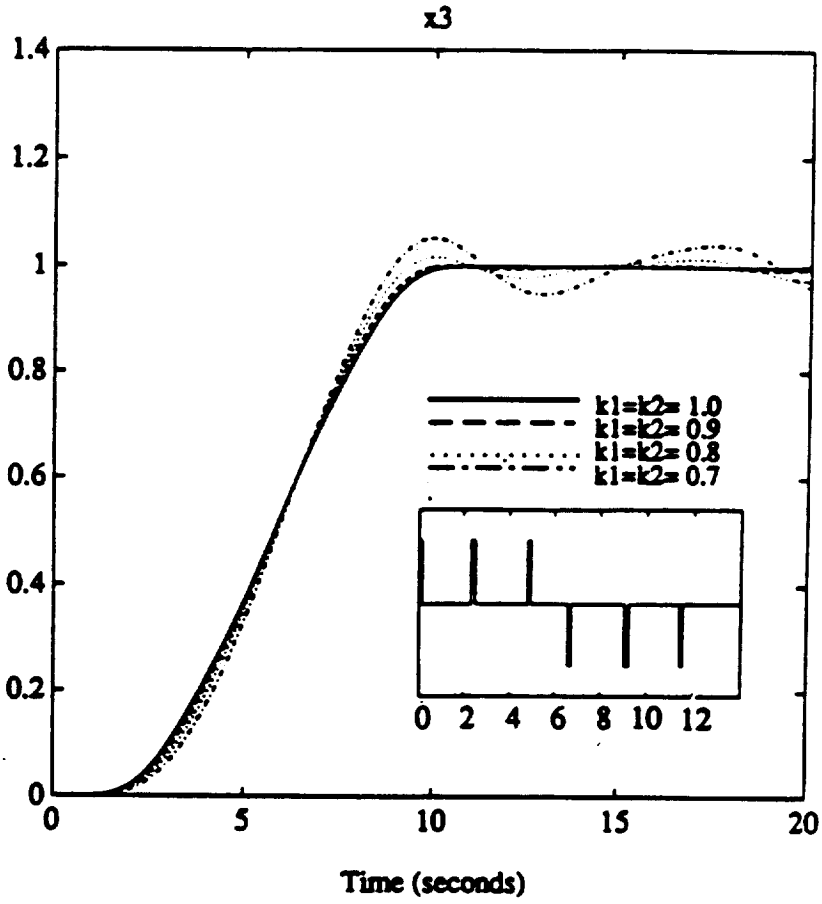

Figure 3.13: Responses to robust fuel and time-optimal control input (Case 2-1).

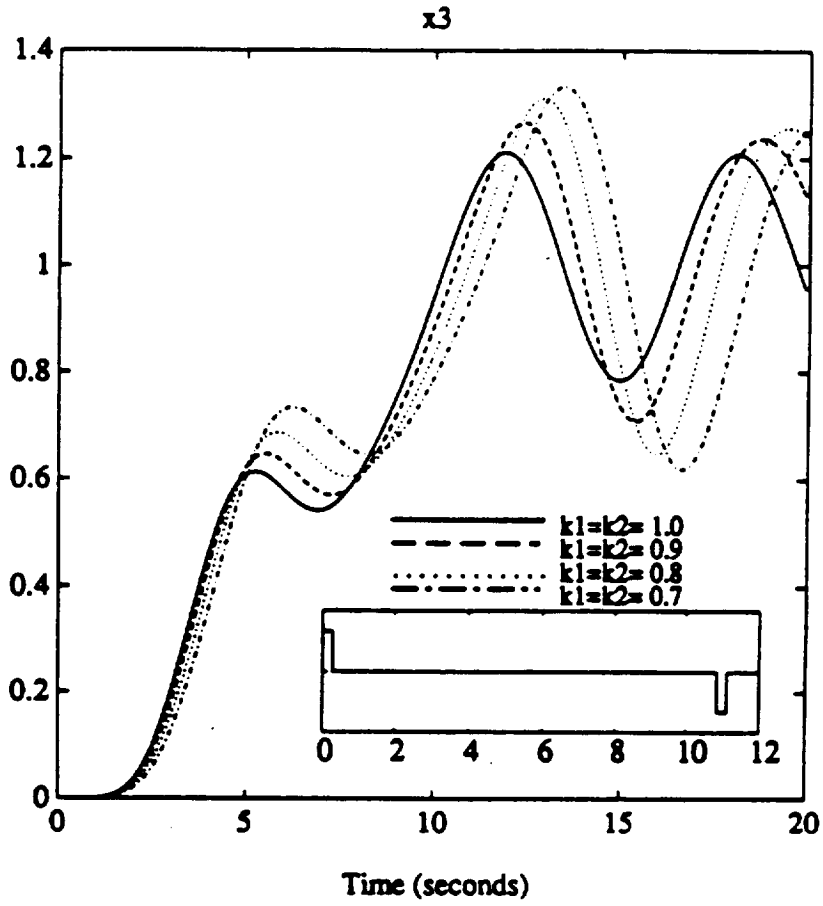

Figure 3.14: Responses to fuel and time-optimal control input (Rigid Body Solution).

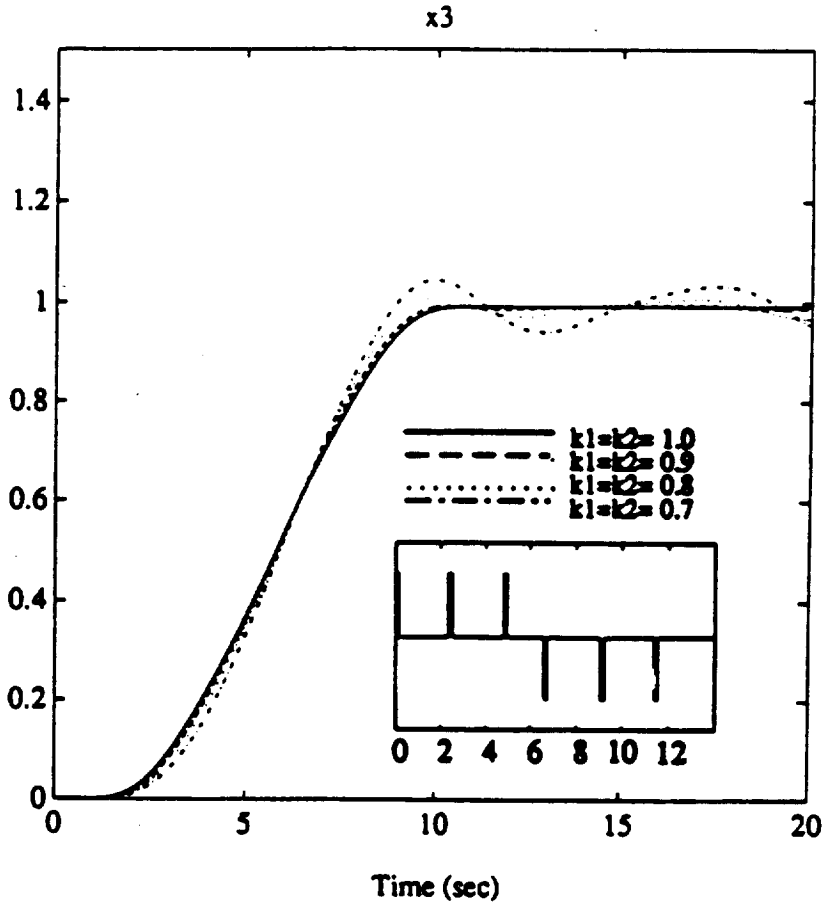

Figure 3.15: Responses to robust fuel and time-optimal control input (Case 2-1).

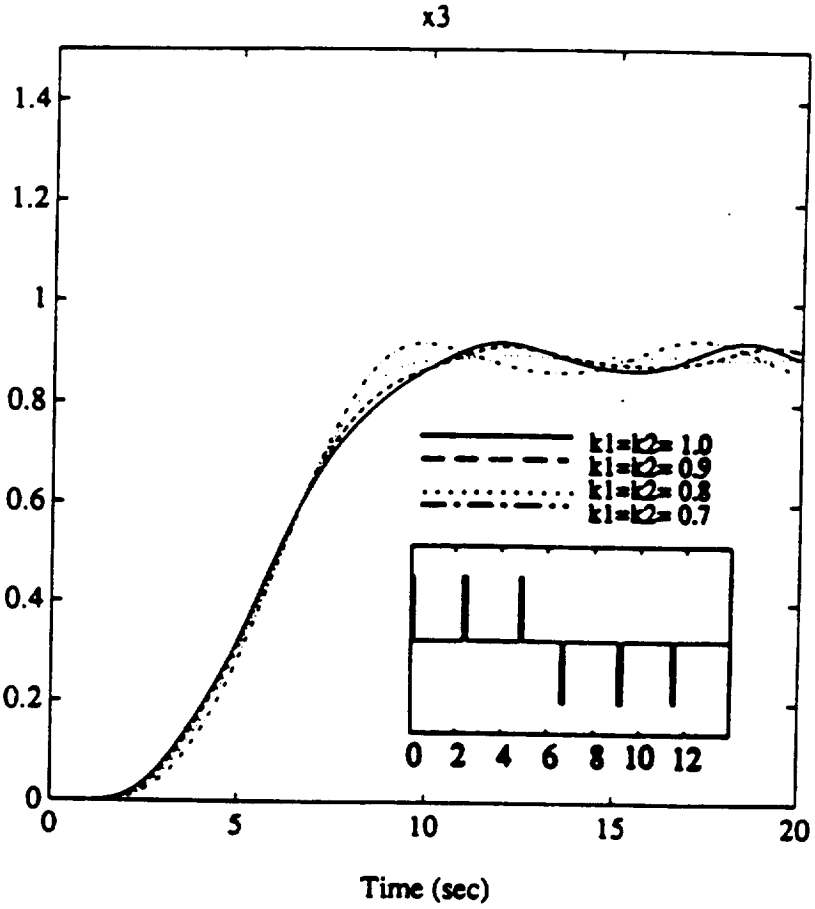

Figure 3.16: Responses to robust fuel and time-optimal control input (Case 2-1).

Chapter 4

Sliding Mode Control Design for Uncertain Flexible Structures

4.1 Introduction

Open-loop controllers do not have feedback information of errors which arise due to uncertainties in the plant. As a result it would be better to use closed-loop feedback controller which should be robust to allow for plant uncertainties. Any feedback design which provides better robustness to parameter variations with no residual vibrations would be a viable alternative to robustified time optimal control logic.

The ultimate goal of the future is to develop feedback control logic for achieving the robust time-optimal performance presented in the earlier chapter. Any scheme should not cause structural excitation and should be robust to parameter variations. The sliding mode control method is used in an attempt to design a controller with the desired properties. The idealized sliding mode control has a high frequency control activity and this is eliminated by the use of boundary layer. The sliding mode control allows for parameter variation of the nominal plant parameters. Since the sliding mode control method does not use bounded controls, a saturator is used to attain bounded controls. The boundary layer concept eliminates chattering by trading off with tracking performance. The good choice of the sliding function which is a weighted sum of the errors enables one to derive a control law. The sliding control method is applicable to

simple systems with decoupled equations of motion. The equations of motion of flexible spacecraft is modelled with the spring mass configuration. The modal equations are decoupled and this makes it possible to obtain the sliding mode controller.

The remainder of this chapter is organized as follows. Section 3.2 describes the variable structure system from which the sliding mode control is developed. Section 3.3 discusses the mathematical details of the sliding mode control theory. The boundary layer method and the robustness to parameter variations as applied to ideal sliding mode control is discussed. In Section 3.4 the benchmark problem of an uncertain flexible structure is defined and the sliding mode control design is shown in Section 3.5. The simulations of the responses are shown for the nominal and perturbed parameters of the model.

4.2 Variable Structure Control

The variable structure control uses switching logic for control. This utilizes functions which would be used as switching functions for switching the control actions to on and off states. This switching function uses information of output feedback.

Consider a system of the form :

$$\dot{x} = f(x,t) + B(x,t)u \tag{4.1}$$

where f and B are matrices and u is the control vector. The components of this vector u is determined by

$$u_i(x,t) = \begin{cases} u_i^+; & s_i(x) > 0 \\ u_i^-; & s_i(x) < 0 \end{cases} \tag{4.2}$$

where $s_i(x)$ is the switching function and u_i^+,u_i^- are the components of control u. The phase plane of the dynamics are utilized in designing the switching

functions to yield the control laws. The sliding mode control has been developed from variable structure control. The variable structure control system has several substructures which may be unstable. Such cases are unacceptable. Sliding mode controller can be obtained as a special case of variable structure control when the right hand side of the equations of motions describing the dynamics has discontinuities on certain surfaces in system phase spaces. The discontinuous control actions of the sliding mode can be viewed as an attraction of phase trajectories onto the sliding surface in phase space. When the trajectory approaches the sliding surface, the perturbations about the surface becomes discontinuous causing high frequency chattering on/off of control states. This is highly undesirable. Sliding mode control provides robustness to parameter variations, robust performance to take care of plant uncertainties and external disturbances.

4.3 Sliding Mode Control Theory

The sliding mode control system is a high gain system and utilizes a high control authority for the tracking problem. The large bandwidth provides a fast settling time. Robust control using a feedback scheme is more effective in treating the plant parameter uncertainties as compared to open loop schemes. The sliding mode control is employed for designing the control law for uncertain flexible structures. The sliding mode control has been developed from the variable structure mode control [22,23,24,25]. The sliding mode control is robust to plant uncertainties and external disturbances. The trajectory of motion of system as illustrated in Fig. 3.1 is causing discontinuity in control action. This is the case when the trajectories are attracted from both regions $\mathcal{G}^+$ and $\mathcal{G}^-$. Once it reaches this discontinuous surface the motion occurs along the surface.

This motion is known as the 'Sliding Mode'. This is the ideal case of sliding mode. The real sliding mode occurs with uncertain plants having parameter variations and unmodelled dynamics. The real sliding causes finite frequency control switches and the trajectory to jump across the discontinuous surface $s_i(x)$. Consider the system

$$\dot{x} = f(x,t,u) \tag{4.3}$$

$$u_i(x,t) = \begin{cases} u_i^+; & s_i(x) > 0 \\ u_i^-; & s_i(x) < 0 \end{cases} \tag{4.4}$$

where $x = [x_1, \ldots . x_n]^T$ are the coordinates of the system, $f = [f_1, \ldots, f_n]^T$ and $u = [u_1, \ldots, u_m]^T$. u_i has discontinuities on the surface $s_i(x) = 0$.

A sliding mode exists for a region of non-zero measure on the surface $s(x) = 0$ if the projections of $f^+ = f(x,t,u^+)$ and $f^- = f(x,t,u^-)$ are of opposite signs on the tangent to the surface and are directed towards it. Also, we have

$$\lim_{s \to 0^-} \dot{s} < 0 \tag{4.5}$$

$$\lim_{s \to 0^+} \dot{s} > 0 \tag{4.6}$$

The solutions of the system of equations with the right hand side discontinuous appears in the sliding mode. Filippov's continuation method is used in this case. The system under consideration is linear with respect to u.

Let G be m × n matrix whose rows are given by

$$\frac{\partial}{\partial x} s_i(x) \equiv [\frac{\partial}{\partial x_1} s_i(x), \ldots, \frac{\partial}{\partial x_n} s_i(x)] \tag{4.7}$$

The equivalent control $\bar{u}$ is obtained as

$$Gf + GB\bar{u} = 0 \tag{4.8}$$

$$\bar{u} = -[GB]^{-1}Gf \tag{4.9}$$

$$\dot{x} = f - B[GB]^{-1}Gf \tag{4.10}$$

provided $[GB]^{-1}$ exists and the initial conditions $s(x(0)) = 0$. This is based on the following property

$$\dot{s}(x) = 0 \tag{4.11}$$

Now consider the case of real sliding mode where the motion occurs near a finite δ vicinity of the manifold $s(x) = 0$;

$$\| s(x) \| \leq \delta, \| s(x) \| = \sqrt{\sum_{i=1}^{m} s_i^2} \tag{4.12}$$

Let $r(s, x)$ be the distance between any point in the neighbourhood and the manifold $s = 0$. It is given by

$$r(s, x) \leq P\delta \tag{4.13}$$

where P is a positive scalar. The real sliding case results in

$$\dot{x} = f(x, t) + B(x, t)\tilde{u}(x, t) \tag{4.14}$$

where $\tilde{u}$ incorporates non-idealities and $B\tilde{u}$ satisfies the Lipschitz conditions (piecewise continuous and bounded). This is in agreement with most real systems.

$$\dot{x} = f^0(x, t) \tag{4.15}$$

$$f^0 = \mu f^+ + (1 - \mu) f^- \tag{4.16}$$

for $0 \leq \mu \leq 1$ and f^0 is a convex hull of f^+ and f^-. Define $\vec{f}_o, \vec{f}_+, \vec{f}_-$ as vectors joining origin to points f^0, f^+, f^- respectively and gradient vector ∇s. From Fig. 3.2 it can be seen that

$$\nabla s \cdot \vec{f}_o = 0 \tag{4.17}$$

Due to frequent switching let the state velocity be f^+ and f^- at time δt_1 and δt_2 respectively. Then substituting

$$\mu = \frac{\delta t_1}{\delta t_1 + \delta t_2} \tag{4.18}$$

into Eqs. (4.16) we get

$$f^0 = (\delta t_1 f^- + \delta t_2 f^-)/(\delta t_1 + \delta t_2) \tag{4.19}$$

i.e., f^0 is the average velocity of motion. Now expanding Eqs. (4.17) we get

$$[\mu f^+ + (1-\mu) f^-](\partial/\partial x)s = 0 \tag{4.20}$$

$$\mu = \frac{f^-(\partial/\partial x)s}{(f^- - f^+)(\partial/\partial x)s} \tag{4.21}$$

Substituting for μ in Eqs. (4.16) we get

$$\dot{x} = [(f^-(\partial/\partial x)s)f^+ - (f^+(\partial/\partial x)s)f^-]/[(f^- - f^+)(\partial/\partial x)s] \tag{4.22}$$

This can be regarded as the sliding mode equations.

Theorem

If

1. On the interval [0, T] any solution $x(t)$ of the system described by Eq.(4.14) is such that the state trajectory is in δ neighbourhood of the manifold $s(x) = 0$, or the inequality (4.12) is valid;

2. For the right hand side of Eq.(4.10) obtained using the equivalent control method

$$x^* = f(x^*,t) - B(x^*,t)[G(x^*)B(x^*,t)]^{-1}G(x^*)f(x^*,t) \tag{4.23}$$

a Lipschitz constant l exist and x^* is a solution of Eq.(4.14);

3. Partial derivatives of the functions $B(GB)^{-1}$ exist and are bounded in any bounded domain.

4. For the right hand side of Eq.(4.14) there exist positive constants q and r such that

$$\| f(x,t) + B(x,t)\tilde{u}(x,t) \| \leq q + r \| x \| \tag{4.24}$$

then for any pair of solutions to Eq.(4.14) and Eq.(4.23) under the initial conditions

$$\| x(0) - x^*(0) \| \leq p\delta \tag{4.25}$$

there exists a positive quantity h such that

$$\| x(t) - x^*(t) \| \leq h\delta \tag{4.26}$$

for $t \in [0,T]$.

The proof the above theorem lies in showing that the ideal sliding and real sliding are close together provided the conditions stated hold. For a real sliding $\dot{s} \neq 0$ as is the case in ideal sliding. The control $\tilde{u}$ will be obtained as

$$\tilde{u} = -(GB)^{-1}Gf + (GB)^{-1}\dot{s} \tag{4.27}$$

and substituting $\tilde{u}$ into Eq.(4.14) we get

$$\dot{x} = f(x,t) - B(x,t)[G(x)B(x,t)]^{-1}G(x)f(x,t) + B(x,t)[G(x)B(x,t)]^{-1}\dot{s} \tag{4.28}$$

The solution of Eq.(4.10) is given by

$$x^*(t) = x^*(0) + \int_0^t \{f(x^*,\tau) - B(x^*,\tau)[G(x^*)B(x^*,\tau)]^{-1}G(x^*)f(x^*,\tau)\}d\tau \tag{4.29}$$

The solution of Eq.(4.28) is given by

$$x(t) = x(0) + \int_0^t \{f(x,\tau) - B(x,\tau)[G(x)B(x,\tau)]^{-1}G(x)f(x,\tau)\}d\tau \tag{4.30}$$

$$+ \int_0^t B(x,\tau)[G(x)B(x,\tau)]^{-1}\dot{s}d\tau \tag{4.31}$$

Now subtracting Eq.(4.31) from Eq.(4.29) gives

$$\begin{aligned} \| x(t) - x^*(t) \| \leq\ & p\delta + \int_0^t l \| x - x^* \| d\tau + \\ & \| B(x,\tau)[G(x)B(x,\tau)]^{-1}s \|_0^t \\ & + \int_0^t \| \frac{d}{d\tau}B(x,\tau)[G(x)B(x,\tau)]^{-1} \| \| s \| d\tau \end{aligned} \tag{4.32}$$

The condition given by Eq.(4.24) and the bounded solution of Eq.(4.31) can be combined as

$$\| x(t) \| \leq \| x(0) \| + mT + \int_0^T n \| x \| dt \tag{4.33}$$

using the Bellman-Gronwall lemma, the above inequality is

$$\| x(t) \| \leq (\| x(0) \| + mT)e^{nT} \tag{4.34}$$

By using the conditions 1-3 of the theorem and inequality Eq.(4.34), we get

$$\| x(t) - x^*(t) \| \leq p\delta + l\int_0^t \| x - x^* \| d\tau \tag{4.35}$$

where p is a positive scalar. Bellman - Gronwall lemma applied on the above inequality gives

$$\| x(t) - x^*(t) \| \leq h\delta \tag{4.36}$$

where ($t \in [0, T]$) and $h = pe^{lT}$. This shows that if initially the actual and ideal states are sufficiently close together, then they remain close over a finite time. This result could also be extended to infinite time interval.

Now consider the exponential stability of linear time invariant systems described by

$$\dot{x} = Ax + Bu + g \tag{4.37}$$

where A and B are constant matrices and disturbance is represented by g. The sliding mode occurs along the intersections of $s_i = 0$ and satisfies

$$\dot{s}_i = CAx + CBu + Cg = 0 \tag{4.38}$$

This results in equivalent control as

$$\bar{u} = -(CB)^{-1}(CAx + Cg) \tag{4.39}$$

which becomes

$$\dot{x}^* = [I - B(CB)^{-1}C]Ax^* + [I - B(CB)^{-1}C]g \tag{4.40}$$

where x^* is the variable of ideal sliding case. In the case of real sliding case the above relations are

$$\tilde{u} = -(CB)^{-1}(Ax + g) + (CB)^{-1}\dot{s} \tag{4.41}$$

$$\dot{x} = [I - B(CB)^{-1}C]Ax + [I - B(CB)^{-1}C]g + B(CB)^{-1}\dot{s} \tag{4.42}$$

The solution of the above two cases can be obtained as :

$$x^*(t) = \Phi(t)x^*(0) - \int_0^t \Phi(t-\tau)[I - B(CB)^{-1}C]g(\tau)d\tau \tag{4.43}$$

$$x(t) = \Phi(t)x(0) - \int_0^t \Phi(t-\tau)[I - B(CB)^{-1}C]g(\tau)d\tau + \int_0^t \Phi(t-\tau)B(CB)^{-1}\frac{ds}{d\tau}d\tau \tag{4.44}$$

where Φ is the state transition matrix. Integrating the above and subtracting them and taking the norms of both sides gives

$$\begin{aligned} \| x(t) - x^*(t) \| \leq & \| \Phi(t) \| \| x(0) - x^*(0) \| + \| B \| \| (CB)^{-1} \| \| s(t) \| \\ & + \| B \| \| (CB)^{-1} \| \| \Phi(t) \| \| s(0) \| \\ & + \int_0^t \| \frac{d}{d\tau} \Phi(t-\tau) B (CB)^{-1} \| \| s \| d\tau \end{aligned} \tag{4.45}$$

For real sliding the inequality $\| s \| \leq \delta$ holds and the functions $\| \Phi(t) \|$ and $\int_0^t \| \frac{d}{d\tau} \Phi(t-\tau) \| d\tau$ are bounded in the infinite time interval for asymptotically stable systems. Then the following inequality holds for positive n

$$\| x(t) - x^*(t) \| \leq n\delta \tag{4.46}$$

and

$$\lim_{\delta \to 0} x(t) = x^*(t) \tag{4.47}$$

for $0 \leq t \leq \infty$.

Now the Filippov's method is applied to the above problem of linear time invariant systems. The convex hull in this case is given by

$$f^0 = f(x,t) + B(x,t) \sum_{i=1}^{2^m} \mu_i u_i \tag{4.48}$$

where $\mu_i \geq 0$ and $\sum_{i=1}^{2^m} \mu_i = 1$. The velocity vector lies on the sliding surface hull and hence $Gf^0 = 0$. Let $z = \sum_{i=1}^{2^m} \mu_i u_i$ and substituting it gives

$$G(f + Bz) = 0 \tag{4.49}$$

or

$$z = -(GB)^{-1} Gf \tag{4.50}$$

which is the identical to Eq.(4.10). Thus the Filipov's method is in agreement to the equivalent control method for the linear time invariant systems. The following conditions hold for attraction to the sliding surface

$$f^+(\partial/\partial x)s \;<\; 0 \;, x \in \mathcal{G}^+ \tag{4.51}$$

$$f^-(\partial/\partial x)s \;>\; 0 \;, x \in \mathcal{G}^- \tag{4.52}$$

which can be combined as

$$\frac{d}{dt}s^2(x;t) < 0 \tag{4.53}$$

which is a local sliding condition. For a proper function $s(x,t)$ and a positive scalar η we have

$$\frac{d}{dt}s^2(x;t) \leq -\eta|s| \tag{4.54}$$

as the global sliding condition for a time varying case. Consider the single-input single-output linear time-varying system

$$x_1^{(n)} + a_{n-1}(t)x_1^{(n-1)} + \ldots + a_0(t)x_1 = u \tag{4.55}$$

Now define the states as $x(t)$ and the desired states $x_d(t)$ as

$$x(t) \;=\; [x_1(t), \dot{x}_1, \ldots, x_1^{(n-1)}(t)] \tag{4.56}$$

$$x_d(t) \;=\; [x_{d1}(t), \dot{x}_{d1}, \ldots, x_{d1}^{(n-1)}(t)] \tag{4.57}$$

$$\tilde{x} \;=\; x(t) - x_d(t) \tag{4.58}$$

Assume

1. $\tilde{x}(0) = 0$

2. $|x_d^{(n+1)}(t)| \leq v$ for all time and constant v

Define the time varying $S(x;t)$, the sliding surface as

$$s(x;t) = C\tilde{x}(t) = 0 \tag{4.59}$$

where $C = [c_1, \ldots . c_{m-1}, 1]$. Now the objective is to obtain control $u(t)$, to make $s(x;t) = 0$. Expanding the above equation we get

$$x_1^{(n-1)} + \sum_{i=0}^{n-2} c_{i+1} x_1^{(i)} = x_{d1}^{(n-1)} + \sum_{i=0}^{n-2} c_{i+1} x_{d1}^{(i)} \tag{4.60}$$

Assumption 1 and the uniqueness of solution of ordinary differential equations would result in

$$x(t) = x_d(t) \ \ \forall t \tag{4.61}$$

Set u as

$$u = \beta^T(x)x + \sum_{i=1}^{n-1} k_i(x;t)\tilde{x}_{i+1} - k_n sgn(s) \tag{4.62}$$

Substituting for control in Eq.(4.55) to get

$$\frac{1}{2}\frac{d}{dt}s^2(x;t) = \sum_{i=1}^{n}(\beta_i(x) - a_{i-1}(t))x_i s + \sum_{i=1}^{n-1}(c_i + k_i(x;t))\tilde{x}_{i+1}s - s x_{d,n+1} - k_n|s| \tag{4.63}$$

The sliding condition results in the constraints

$$\beta_i(x) \equiv \beta_i^+ \leq a_{i-1}(t), x_i s > 0 \ \ \forall t, i = 1, \ldots, n \tag{4.64}$$

$$\beta_i(x) \equiv \beta_i^- \geq a_{i-1}(t), x_i s < 0 \ \ \forall t, i = 1, \ldots, n \tag{4.65}$$

$$k_i(x;t) \equiv k_i^+ \leq -c_i, \tilde{x}_{i+1} s > 0 \ \ \forall t, i = 1, \ldots, n-1 \tag{4.66}$$

$$k_i(x;t) \equiv k_i^- > c_i, \tilde{x}_{i+1} s < 0 \ \ \forall t, i = 1, \ldots, n-1 \tag{4.67}$$

$$k_n > v \tag{4.68}$$

When $c_i = 0$ for some i, corresponding $k_i\tilde{x}_{i+1}$ is set to zero. The discontinuities are at

$$x_i = 0; \tilde{x}_j = 0, s = C\tilde{x} = 0 \tag{4.69}$$

but control is discontinuous only at $s(t) = 0$. Combining Eq(4.54) and Eq(4.63)

$$\frac{1}{2}\frac{d}{dt}s^2(x;t) \leq -(k_n - v)|s| \tag{4.70}$$

for all t.

Parameter variations in sliding mode control is incorporated in the constraints. Consider the finite bounds of parameter variations of a_i as

$$\alpha_i \leq a_i(t) \leq \gamma_i, \quad i = 0, \ldots, n \tag{4.71}$$

Then from Eq(4.64)-Eq(4.67) we get

$$\beta_i^+ \leq \alpha_{i-1} \tag{4.72}$$

$$\beta_i^- \geq \gamma_{i-1} \tag{4.73}$$

for $i = 1, \ldots, n$, control yields $x(t) = x_d(t)$. To incorporate robustness to external disturbance given by

$$d(x;t) = [0, \ldots, 0, d_1(x,t)]^T \tag{4.74}$$

$$|d_1(x;t)| \leq \sum_{i=1}^{n} \delta_i |x_i| + \delta_0 \tag{4.75}$$

The control law given by Eq(4.63) will yield $x(t) = x_d(t)$ as long as

$$\beta_i^+ \leq \alpha_{i-1} - \delta_i \tag{4.76}$$

$$\beta_i^- \geq \gamma_{i-1} - \delta_i, i = 1, \ldots, n \tag{4.77}$$

$$k_n > v + \delta_0 \tag{4.78}$$

are satisfied. The initial condition assumption, $x_d(0) \neq x(0)$, may be true and this implies that the points in hyperspace may not be on the sliding surface. But using the control law, the offset will asymptotically approach zero provided

Eq(4.60) is stable. Let the class of nonlinear time-varying systems described by

$$\theta_j^{(n_j)} = f_j(\Theta_1, \Theta_2, \ldots, \Theta_p; t) + u_j, \quad j = 1, \ldots, p \tag{4.79}$$

where, for $i = 1, \ldots, p$ and $\Theta_j = [\theta_i, \dot{\theta}_i, \ldots, \theta_i^{n_i-1}]^T$. The tracking problem is to make θ_j approach θ_{dj}. Define the tracking error as $\tilde{\Theta}_j(t) = \Theta_j(t) - \Theta_{dj}(t)$. Now replace the discontinuous control by the continuous control law

$$s_j(\Theta_j; t) = C_j \tilde{\Theta}_j(t) \tag{4.80}$$

Define a boundary layer about the sliding surface as

$$s_j^-(\Theta_j; t) \doteq s_j(\Theta_j; t) + C_{j1}\epsilon_j \tag{4.81}$$

$$s_j^+(\Theta_j; t) \doteq s_j(\Theta_j; t) - C_{j1}\epsilon_j \tag{4.82}$$

where $C_{j1} > 0$ and ϵ_j is the hyper-radius of boundary layer. The boundary layer $\mathcal{B}_j(t)$ is defined by

$$\mathcal{B}_j(t) = \{\Theta : s_j^-(\Theta_j; t) > 0 | s_j^+(\Theta_j; t) < 0\} \tag{4.83}$$

$$\frac{d}{dt}s_j^- = \frac{d}{dt}s_j = \frac{d}{dt}s_j^+ \tag{4.84}$$

Choose $u_j(\Theta, t)$ so that outside $\mathcal{B}_j$ we have

$$\frac{d}{dt}s_j^- > 0 \; \forall \Theta \in s_j^-(t) \tag{4.85}$$

$$\frac{d}{dt}s_j^+ < 0 \; \forall \Theta \in s_j^+(t) \tag{4.86}$$

The boundary layer is the attraction for points in hyperspace which is assured by the above conditions. Any continuous interpolations between u_j for s^- and u_j for s^+ will suffice. If

$$s_j = (\frac{d}{dt} + \lambda_j)^{n_j-1}(\theta_j - \theta_{dj}), \lambda_j > 0 \tag{4.87}$$

then with $\Theta_j(0) = \Theta_{dj}(0)$

$$|\Theta_j - \Theta_{jd}| \leq \epsilon_j \forall t \geq 0 \tag{4.88}$$

If $\Theta_j(0) \neq \Theta_{dj}(0)$, we have

$$|\Theta_j - \Theta_{jd}| \leq \epsilon_j + P(t) \parallel \tilde{\Theta}_j(0) \parallel \exp(-\lambda t) \tag{4.89}$$

where $P(t)$ is a polynomial in t.

Consider the single-input single-output system of the form

$$\begin{aligned} \dot{x}_1 &= x_2 \\ \dot{x}_2 &= x_3 \\ &\vdots \\ \dot{x}_n &= f(x) + g(x)u + d \end{aligned} \tag{4.90}$$

where the states are $x = [x_1\ x_2\ \ldots\ x_n]^T$, u is the control, y is the output and d the disturbance. The tracking problem is to make output approach the desired output while allowing for uncertainties in f and g. The time varying sliding surface s is defined as

$$s(x;t) = (\frac{d}{dt} + \lambda)^{n-1}\tilde{x}, \ \ \lambda > 0 \tag{4.91}$$

where $e = y_d - y$ and λ is constant scalar. The trajectories are attracted to the sliding surface and this results in nullifying the error. The phase plane trajectory should converge to the sliding surface in order for the control law to be effective in fulfilling the desired tracking objective. Chattering is removed by smoothing out the control surface discontinuity in a thin boundary layer neighbouring the switching surface which is given by

$$\mathcal{B}(t) = \{x : \ |s(x;t)| \leq \lambda^{n-1}\epsilon\} \tag{4.92}$$

where the thickness of the boundary layer $\epsilon > 0$. Consider the modelling error

$$f = \hat{f} + \delta f \tag{4.93}$$

Assume that

$$|\delta f| \leq F \tag{4.94}$$

$$|d| \leq D \tag{4.95}$$

where $\hat{f}$, F and D are known functions of time and states. Let

$$k(x;t) = h(x,t) + d(x,t) + v(t) + \eta \geq \eta > 0 \tag{4.96}$$

$$u = -\hat{f} - \sum_{p=1}^{n-1} C_p^{n-1} \lambda^p \tilde{x}^{n-p} - k(x;t) sgn(x) \tag{4.97}$$

Introduce a boundary layer of thickness ϵ, and thereby modifying the control to

$$u = -\hat{f} - \sum_{p=1}^{n-1} C_p^{n-1} \lambda^p \tilde{x}^{n-p} - k \ \ sat(\frac{s}{\lambda^{n-1}\epsilon}) \tag{4.98}$$

where *sat* is the saturator and this control does satisfy the sliding condition Eqs.(4.54). For points satisfying $\tilde{x}(0) = 0$,

$$\dot{s} = k(x;t)\frac{s}{\lambda^{n-1}\epsilon} + (\delta f(x,t) + d(t) - x_d^{(n)}) \tag{4.99}$$

$$= k(x_d;t)\frac{s}{\lambda^{n-1}\epsilon} + (\delta f(x_d,t) + d(t) - x_d^{(n)} + O(\epsilon)) \tag{4.100}$$

for δf and k are continuous functions.

The sliding condition that needs to be satisfied for convergence is

$$\frac{1}{2}\frac{d}{dt}(s^2) \leq -\eta|s| \tag{4.101}$$

for a non-negative constant η. This condition is like a Lyapunov function. It shows that the distance squared from the sliding surface (s^2 term), gets smaller as the trajectories are traversed toward the sliding surface. The sliding surface

also allows for disturbances and uncertainties like parameter variations and the sliding condition takes care of the perturbation caused. Control laws which satisfy the sliding condition are discontinuous across the sliding surface and lead to control chattering. This is due to the absence of the exact knowledge of the value of the sliding variable. This leads to jumps across the sliding surface at high frequency. This is the phenomenon behind high frequency chattering. Chattering can excite higher order modes. Thus it lowers the robustness to unmodelled dynamics which are the higher modes. Hence it would be desirable to smoothen the control and eliminate chattering.

In case of $g(x) = b$ (scalar constant), let b vary in the interval given by

$$0 < b_{min} \leq \quad b \quad \leq b_{max} \tag{4.102}$$

This bounded interval margin is assumed to contain the parameter variations of parameter b. This should take care of robustness to parameter variations in b, the control gain constant that appears in the equations of motion of the system. This interval margin is bounded and represents a function of masses and spring stiffness in the case of flexible structures. Hence the variations in b are caused by variations of real parameter variations like masses and spring stiffness which are uncertain parameters. The control gain b appears as a product in the equations of motion and this results in multiplicative uncertainty. Define

$$\hat{b} = (b_{min} b_{max})^{\frac{1}{2}} \tag{4.103}$$

$$\beta = (b_{min}/b_{max})^{\frac{1}{2}} \tag{4.104}$$

β is the analogue of gain margin in linear control and $\hat{b}$ is the geometric mean

of extreme bounds of b. The perfection in tracking is achieved by

$$\lambda^n \epsilon = \beta k_{max} \tag{4.105}$$

In the case of time varying boundary layer the control is chosen to satisfy

$$\frac{1}{2}\frac{d}{dt}s^2 \leq -\eta|s| + \lambda^{n-1}\dot{\epsilon}|s| + \lambda^{n-1}|\dot{\epsilon}s|(\beta - 1) \tag{4.106}$$

The corresponding dynamics of boundary layer thickness are

$$k(x_d;t) \geq \lambda^n \epsilon/\beta \;\Rightarrow\; \dot{\epsilon} + \lambda\epsilon = \frac{\beta}{\lambda^{n-1}}k(x_d;t) \tag{4.107}$$

$$k(x_d;t) \leq \lambda^n \epsilon/\beta \;\Rightarrow\; \dot{\epsilon} + \frac{\lambda\epsilon}{\beta^2} = \frac{1}{\beta\lambda^{n-1}}k(x_d;t) \tag{4.108}$$

$$\epsilon(0) = \frac{\beta}{\lambda^n}k(x_d(0),0) \tag{4.109}$$

$$\overline{k}(x;t) = [k(x;t) - k(x_d;t)] + \lambda^n\epsilon(t)/\beta \tag{4.110}$$

The control law is given by

$$u = \hat{b}^{-1}[\hat{u} - ksgn(s)] \tag{4.111}$$

The sliding condition is satisfied and this represents the analogue of the switching function of variable structure control. The control law takes into account parameter variations in b. Chattering is greater and it would be desirable to smoothen the control action. This smoothening should keep useful properties of robustness to parameter variations, robustness performance and good tracking properties of sliding mode control. Slotine and Sastry [22] have developed a boundary layer to eliminate chattering. Redefining the boundary layer ϕ as

$$\phi(t) = \lambda^{n-1}(t)\epsilon(t) \tag{4.112}$$

modifies the control to the following form

$$u = -\hat{f} - \sum_{p=1}^{n-1} C_p^{n-1}\lambda^{p-1}(\lambda x^{(n-p)} + p\dot{\lambda}x^{n-p-1}) - \overline{k}(x;t)\ sat(\frac{s}{\phi}) \tag{4.113}$$

C-2

The boundary layer is space surrounding the sliding surface in an envelope in the hyperspace. This contains the discontinuity jumps which take place and could be thought of as an analogue of a dead zone. The undesirable chattering is eliminated. The action of boundary layer is similar to that of a low pass filter near the sliding surface to variable s. A trade off between tracking and robustness to parameter variations results. The tuning parameter is the thickness of the boundary layer. A time-varying boundary layer is utilized to allow for variations of boundary layer with time. In the case of time varying boundary layer, the dynamics are given by

$$k(x_d) \geq \lambda\phi/\beta_d \quad \Rightarrow \quad \dot{\phi} + \lambda\phi = \beta_d k(x_d) \tag{4.114}$$

$$k(x_d) \leq \lambda\phi/\beta_d \quad \Rightarrow \quad \dot{\phi} + \lambda\phi/\beta_d^2 = k(x_d)/\beta_d \tag{4.115}$$

where

$$\bar{k} = k(x) - k(x_d) + \lambda\phi/\beta_d \tag{4.116}$$

and x_d is the desired target state x. The initial condition is

$$\phi(0) = \beta_d k(x_d(0))/\lambda \tag{4.117}$$

4.4 Model of an Uncertain Flexible Structure

Consider the two mass-spring system shown in Fig. 3.3 which is a generic model of an uncertain dynamical system with one rigid body mode and one vibration mode [26] . The equation of motions can be written as :

$$\begin{bmatrix} \dot{x}_1 \\ \dot{x}_2 \\ \dot{x}_3 \\ \dot{x}_4 \end{bmatrix} = \begin{bmatrix} 0 & 0 & 1 & 0 \\ 0 & 0 & 0 & 1 \\ -k/m_1 & k/m_1 & 0 & 0 \\ k/m_2 & -k/m_2 & 0 & 0 \end{bmatrix} \begin{bmatrix} x_1 \\ x_2 \\ x_3 \\ x_4 \end{bmatrix} + \begin{bmatrix} 0 \\ 0 \\ 1/m_1 \\ 0 \end{bmatrix} u \tag{4.118}$$

$$y = x_2 \tag{4.119}$$

where x_1 and x_2 are the positions of body 1 and body 2, respectively; x_3 and x_4 are the velocity of body 1 and body 2 respectively. The aim is to design a feedback controller for a unit step output command tracking problem for the controlled output x_2 with the following specifications :

1. Control input is limited as $|u| \leq 1$.

2. Performance requirements : settling time and overshoot are both to be minimized.

3. Performance robustness and stability robustness with respect to the uncertain parameters m_1. m_2 and k (with nominal values of $m_1 = m_2 = k = 1$) are to be maximized.

The equations of motion can be written in modal coordinates as :

$$\ddot{y}_1 = \phi_1 u \tag{4.120}$$

$$\ddot{y}_2 + \omega^2 y_2 = \phi_2 u \tag{4.121}$$

where ω is the natural frequency of the vibration mode and ϕ_1 , ϕ_2 are the gain constants.

4.5 Sliding Mode Controller Design

The initial conditions for the rest-to-rest maneuver is

$$y_1(0) = y_2(0) = 0 \tag{4.122}$$

$$\dot{y}_1(0) = \dot{y}_2(0) = 0 \tag{4.123}$$

and the final conditions

$$y_{1d} = 1, y_{2d} = 0 \tag{4.124}$$

$$\dot{y}_{1d} = 0, \dot{y}_{2d} = 0 \tag{4.125}$$

The sliding surface is to be defined in terms of sliding variable s. Let

$$s = \dot{\tilde{y}}_1 + \lambda \dot{\tilde{y}}_2 \tag{4.126}$$

where $\tilde{y} = y - y_d$. The parameter λ is the weight used in the error function and it also acts as the poles of the filter in the dynamics of the sliding variable. Thus the problem is reduced to a tracking problem to satisfy the rest-to-rest maneuver. By approaching the sliding surface in the phase space would be the strategy of the controller for achieving perfect tracking. Differentiating s, we get

$$\dot{s} = u(\phi_1 + \lambda\phi_2) - \lambda\omega^2 y_2 - \ddot{\tilde{y}}_{1d} - \lambda\ddot{\tilde{y}}_{2d} \tag{4.127}$$

where $\ddot{\tilde{y}}_d$ is the desired target acceleration.

The control logic u is of the form

$$u = a\{\hat{u} - ksgn(s)\} \tag{4.128}$$

where

$$\hat{u} = a[\lambda\hat{\omega}^2 y_2 + \lambda\ddot{\tilde{y}}_{2d} + \ddot{\tilde{y}}_{1d}] \tag{4.129}$$

$$a = (\hat{\phi}_1 + \lambda\hat{\phi}_2)^{-1} \tag{4.130}$$

and the $\hat{\omega}, \hat{\phi}_1, \hat{\phi}_2$ are the worst case parameter variations. This is introduced to make the control robust to parameter variations in masses $m1$ and $m2$ and spring stiffness k.

To satisfy the sliding mode condition

$$s\dot{s} \leq -\eta|s| \tag{4.131}$$

the following condition need to hold

$$k \geq -\frac{a}{\phi_1 + \lambda\phi_2}[-\eta + |\lambda\omega^2 y_2 + \ddot{\tilde{y}}_{1d} + \lambda\ddot{\tilde{y}}_{2d}|] + |a\lambda\hat{\omega}^2 y_2| + |A(\ddot{\tilde{y}}_{1d} + \lambda\ddot{\tilde{y}}_{2d})| \tag{4.132}$$

This sets the lower bound on the value of K to be chosen. Now the boundary layer ϕ is included to modify the control law to

$$u = \{\hat{u} - \overline{k} sat(s/\phi)\} \tag{4.133}$$

To satisfy the bounded control specification we saturate it as

$$u \leftarrow sat(u) \tag{4.134}$$

Carrying out the simulations the results for the above example yields a sluggish response. The response has considerable fluctuations and would result in large settling time larger than 10 seconds. It shows some chattering activity initially which is undesirable. By using

$$s = \tilde{y}_1 + \lambda \tilde{y}_2 \tag{4.135}$$

and using the same control law obtained before we obtain the better response shown in Fig. 3.4. This design has settling time of about 8 seconds and is simulated for the exact nominal case of parameters. It has a small overshoot and it has no chattering or any residual vibrations. The control time history also shows the switching of control to both extremes and also the linear variations combinations. The rise time is fast and these are the desirable properties required for a control design.

This control design should be robust to parameter variations. Now the parameter variations are introduced and the simulation results are shown for various values of parameter variations in the Fig. 3.5-3.8. This illustrates the robustness to parameter variation and stability robustness. The ability of the controller to switch and provide the necessary control action is seen clearly in these simulations. Further the variations in the control actions to different cases of parameter variations are seen. This is in contrast to the robustified

time optimal solutions where one control time history had to be used for any case of parameter variations.

4.6 Conclusion and Issues

An observor can be designed for estimating one of the states the position of the first mass. However the methodology used in the design of the sliding mode controller is to convert to modal coordinates. The transformation from real coordinates to modal coordinates needs the knowledge of both the states. The sliding mode controller is a nonlinear scheme which also provides robustness to parameter variations and robust performance. Its introduction to a generic case of uncertain flexible structures has been shown to provide a good performance.

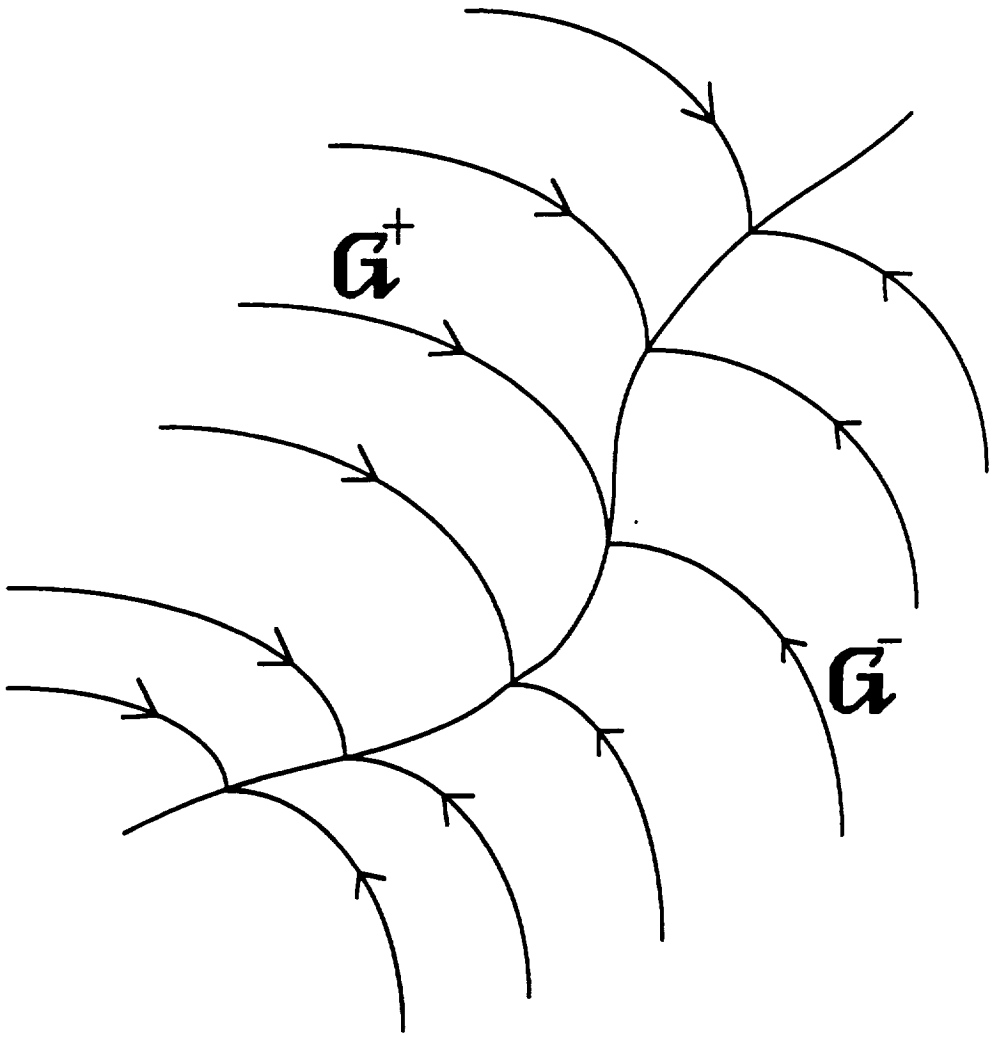

Figure 4.1: Sliding Mode Region.

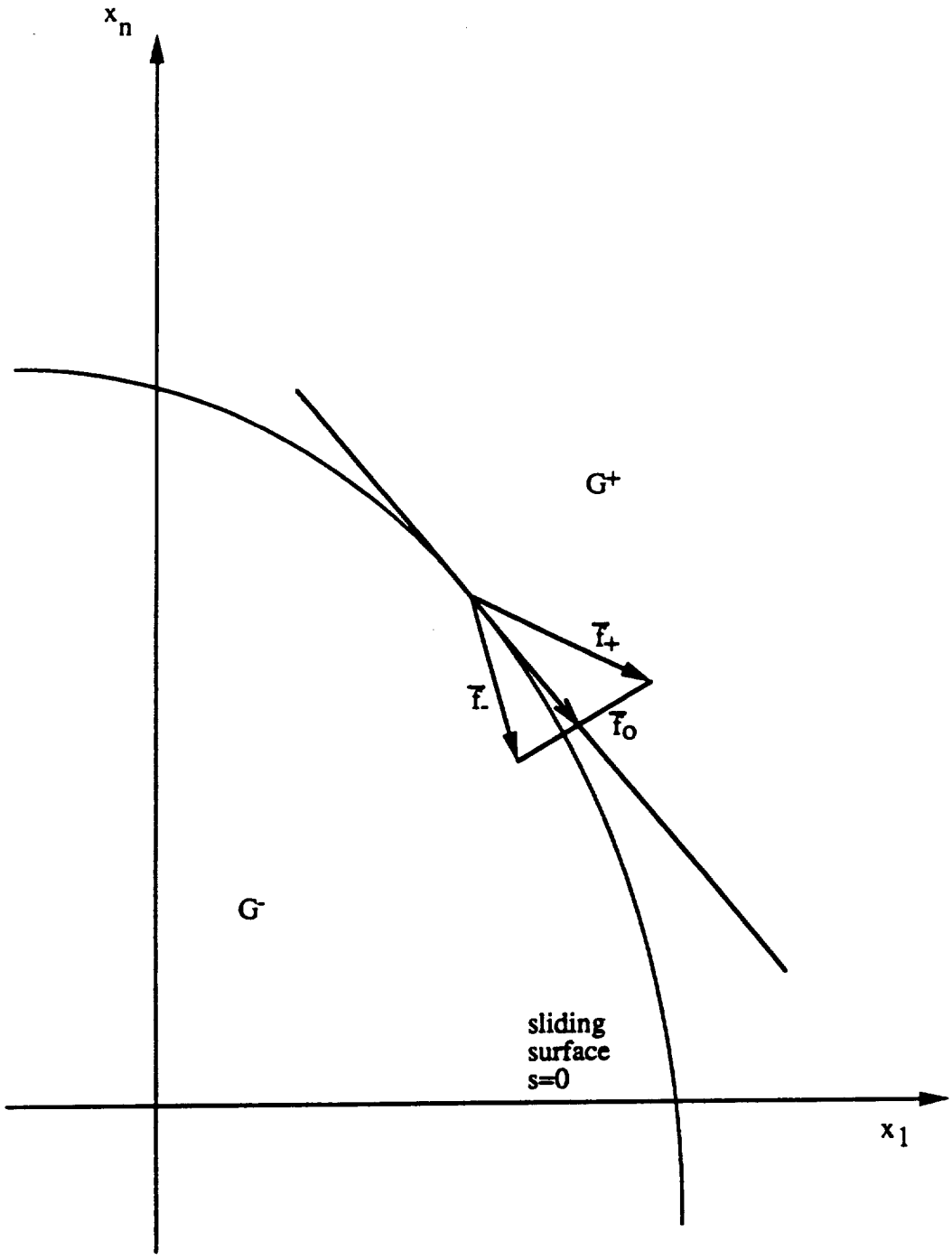

Figure 4.2: Sliding surface.

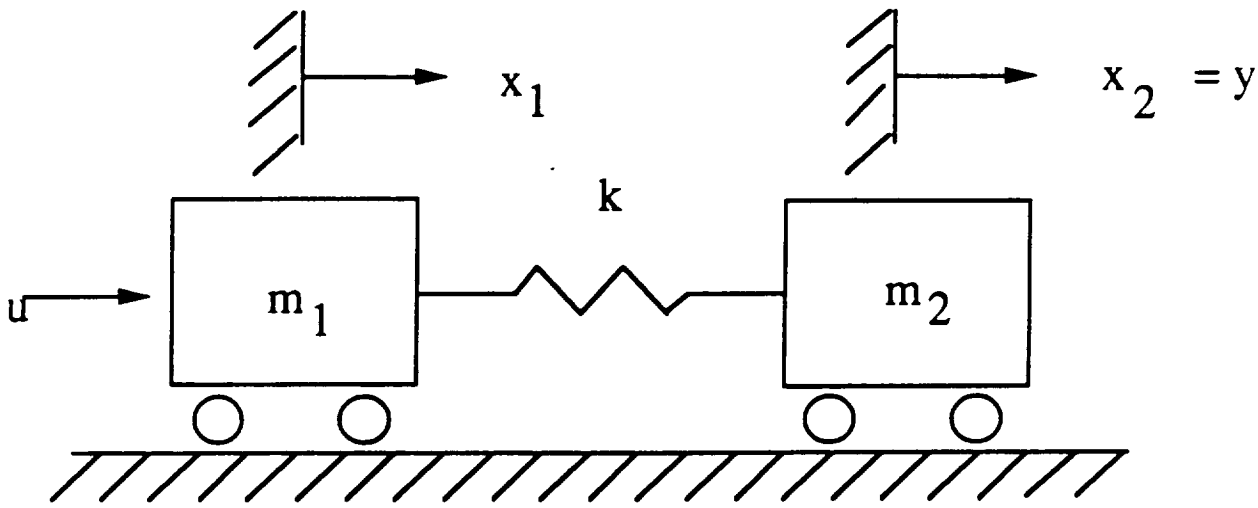

Figure 4.3: Math model of two-mass-spring dynamical system

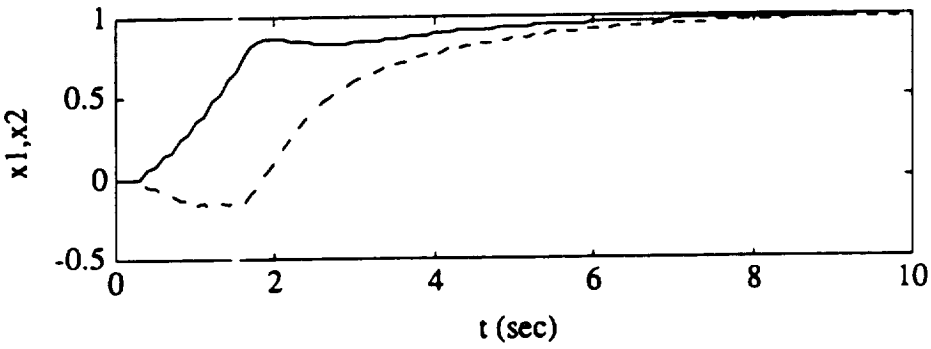

(a) Response

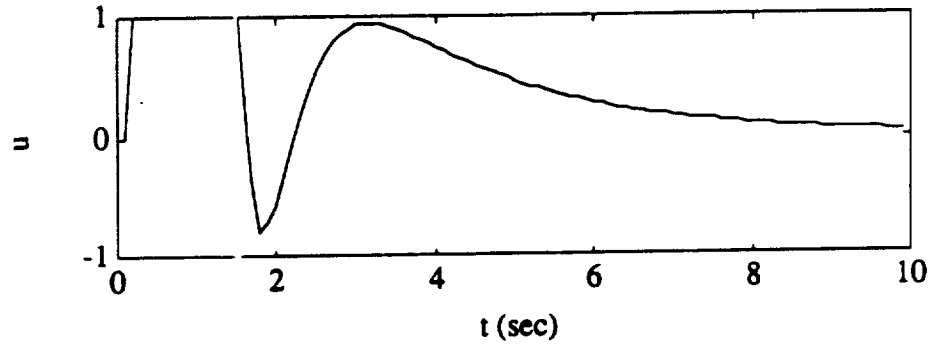

(b) control

Figure 4.4: Response and control of sliding mode controller for the case with parameters k =1 , m1 = 1 , m2 = 1 (nominal case).

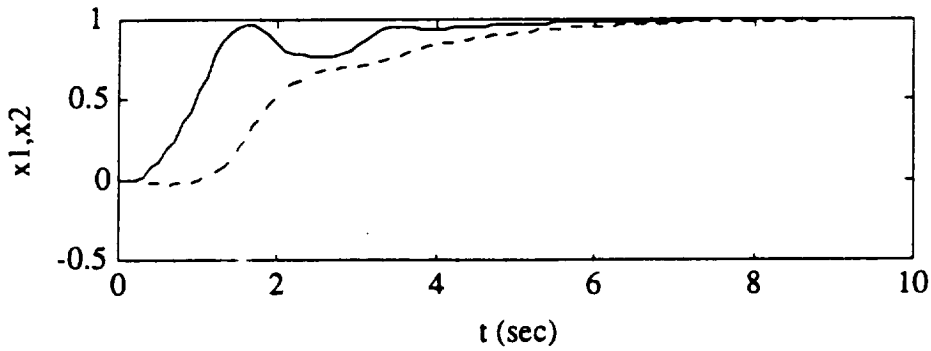

(a) Response

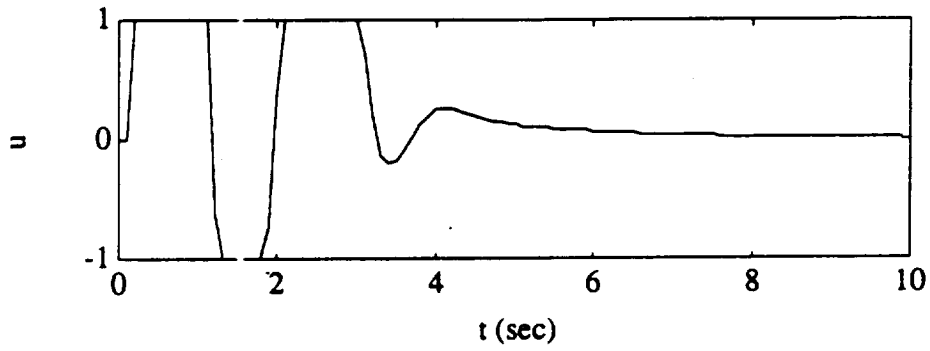

(b) control

Figure 4.5: Response and control of sliding mode controller for the case with parameters k =1 , m1 = 0.5 , m2 = 0.5 .

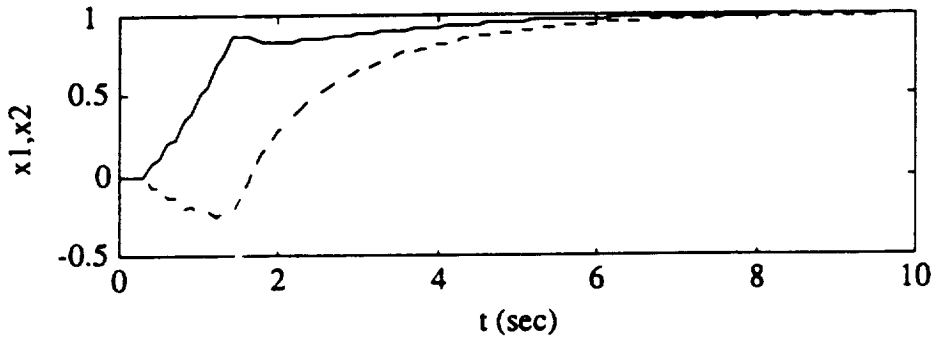

(a) Response

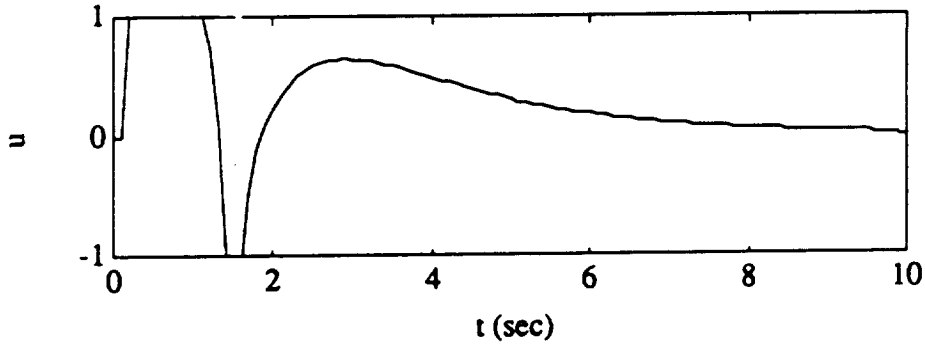

(b) control

Figure 4.6: Response and control of sliding mode controller for the case with parameters k = m1 = m2 = 0.7 .

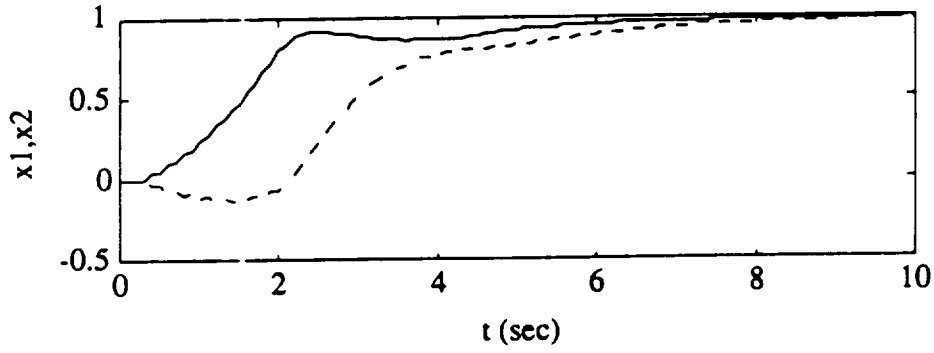

(a) Response

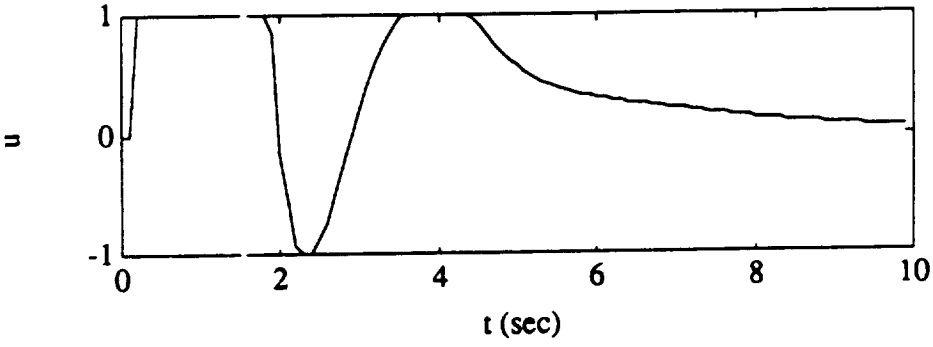

(b) control

Figure 4.7: Response and control of sliding mode controller for the case with parameters k =1 , m1 = 1.5 , m2 = 1.5 .

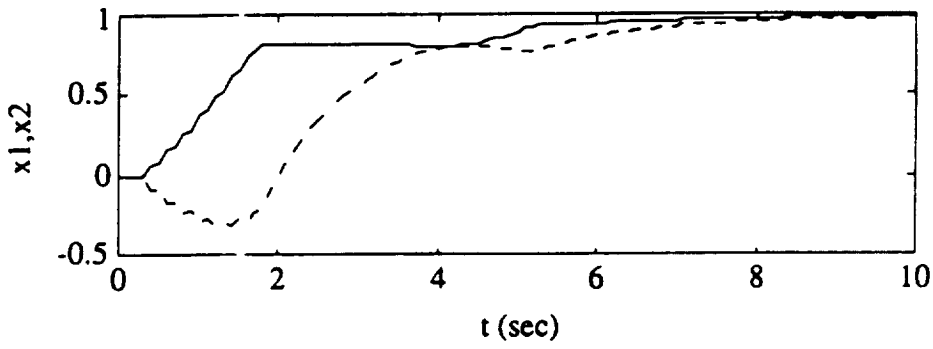

(a) Response

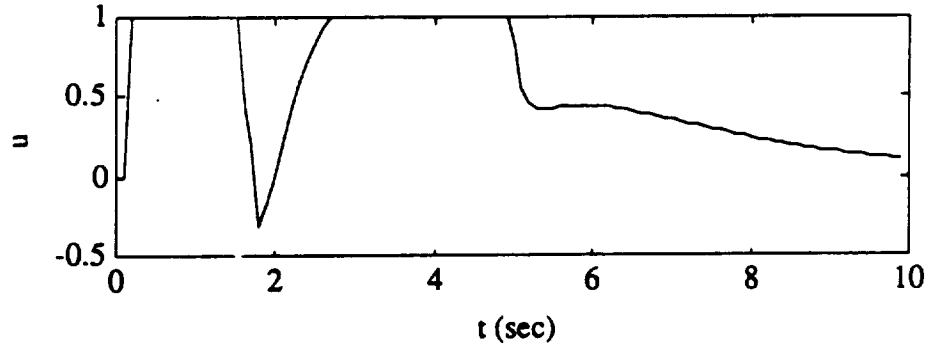

(b) control

Figure 4.8: Response and control of sliding mode controller for the case with parameters k =1 , m1 = 1 , m2 = 0.7 .

Chapter 5

Conclusion

The robust time-optimal open-loop control problem of flexible spacecraft in the face of modeling uncertainty has been investigated. The primary study objective was to explore the feasibility of computing open-loop, on-off pulse control logic for uncertain flexible spacecraft. The results indicate that the proposed approach significantly reduces the residual structural vibrations caused by modeling uncertainty. The results also indicate the importance of a proper jet placement for practical trade-offs among the maneuvering time, fuel consumption, and performance robustness. It is shown that most problems require an accurate mathematical model and thus are sensitive model parameter variations. A nonlinear constrained parameter optimization method is used for solving this problem. The structural flexibility and mass distribution of the vehicle is uncertain while the total mass is well known. So the uncertainty occurs in modal frequency and mode shapes. The case of one sided control inputs only satisfies the necessary conditions and theorems on uniqueness and structure of controls do not exist at this time. The time-optimal responses are shown to be quite sensitive to variations in model parameters. The response of displacement of masses due to variation of spring stiffness is illustrated. Similar responses can also be observed for arbitrarily combined variations of k_i and m_i but keeping total mass constant. The two one-sided control inputs solutions are bang-off-bang nature and in this case the control on-time is not equal to the maneuver time as was the case in bang-bang control. This shows

saving in fuel consumption even though the objective function does not have any weighted fuel terms. The robustness constraints are incorporated and the parameter optimization problem is solved with these constraints. The number of pulses are increased to match the additional number of constraints. The results indicate that the robust time-optimal solution are less sensitive to parameter variations. The performance robustness increases at the expense of increased maneuver time. By prolonging maneuver time does not reduce residual vibrations caused by model uncertainty but a properly coordinated pulse sequences, the flexible modes are not significantly excited during maneuver and are well desensitized. The summary in chapter 2 shows that case 2-3 was the best actuator location in terms of overall performance. The accuracy of the switching time is also presented and it is shown that the robust time-optimal solution is insensitive to parameter variations for switching time accuracy upto two places of decimal. The problem of solving the optimal actuator location using m thrusters in an n mass spring configuration is still an open research problem.

The robust fuel- and time-optimal control of uncertain flexible spacecraft have also been investigated. The consumed fuel was assumed to be small compared to the mass of the spacecraft and it was assumed to be proportional to the jet on-time. The performance index is a weighted function of the maneuver time and jet on-time. The bang-off-bang nature of the two one sided control provides a considerable reduction of jet on-time. It is again noticed in the fuel- and time-optimal control solution that the total maneuver time in not the same as the jet on-time. The rigid body solution is shown to have significant residual vibration and hence it is necessary to include flexible modes. The robust fuel- and time-optimal control again shows increased maneuvering time at the expense of robustness. It was shown that by obtaining a rigid body

solution with comparable final time with the robust fuel- and time-optimal solution of flexible structure, the residual vibrations are siginificant larger in the rigid body solutions.

The sliding mode control design using bounded control inputs was obtained for the benchmark problem. The results indicate robust performance to parameter variations. The feedback design uses a saturator to bound the control inputs. The stability of such controller was not studied and it remains an open issue. This scheme is not minimizing the maneuvering time or the fuel consumption. The fast settling time and low overshoot are the characterstics shown by this design.

There are some limitations of the present work. The analysis is restricted to linear, elastic and undamped systems. The future research directions should be towards the ultimate goal to develop nonlinear feedback control for achieving the robust fuel- and time-optimal performance. The experimental verification of the applicability of the robust fuel- and time-optimal control should provide more insight in its practical implementation. The mathematical rigorous conditions are also needed for necessary and sufficient conditions of time-optimal control in the case of two one-sided controls.

REFERENCES

[1] L. S. Pontrygin, V. G. Boltyanski, R. V. Gamkreledze and E. F. Mischenko, "The Mathematical Theory of Optimal Processes," *Interscience Publishers*, 1962, pp 27.

[2] J. Ben-Asher. J. A. Burns, and E. M. Cliff, "Time-Optimal Slewing of Flexible Spacecraft," *Proceeding of the 26th IEEE Conference on Decision and Control*, 1987, pp.524-528.

[3] G. Singh, P. T. Kabamba, N. H. McClamroch, "Planar, Time-Optimal, Rest-to-Rest Slewing Maneuvers of Flexible Spacecraft," *Journal of Guidance, Control and Dynamics*, Vol. 12, No. 1, 1989, pp.71-81.

[4] G. Singh, P. T. Kabamba, N. H. McClamroch, "Time-Optimal Slewing Maneuvers of Rigid Body with Flexible Appendages," *Proceeding of the 26th IEEE Conference on Decision and Control*, 1987, pp.1441-1442.

[5] E. Barbier and U. Ozguner, "Rest-to-Rest Slewing of Flexible Structure in Minimum Time," *Proceeding of the 27th IEEE Conference on Decision and Control*, 1988, pp.1633-1638.

[6] L. Y. Pao and G. F. Franklin, "Time-Optimal Control of Flexible Structures," *Proceeding of the 29th IEEE Conference on Decision and Control* December 1990, pp. 2580-2581.

[7] S. B. Skaar, L. Tang and Y. Yalda-Mooshabad, "On-Off Attitude Control of Flexible Satellite," *Journal of Guidance, Control and Dynamics*, Vol. 9, July-Aug. 1986, pp.507-510.

[8] D. M. Aspinwall, "Acceleration Profiles for Minimizing Residual Response," *ASME Journal of Dynamic Systems, Measurement, and Control*, Vol. 102, No. 1, 1980, pp.3-6.

[9] C. J. Swigert, "Shaped Torque Techniques," *Journal of Guidance, Control and Dynamics*. Vol. 3, No.5, 1980, pp.460-467.

[10] P. H. Meckl and W. P. Seering, "Active Damping in a Three-Axis Robotic Manipulator," *Journal of Vibration, Acoustics, and Stress and Reliability in Design*, Vol. 107, Jan. 1985, pp.38-46.

[11] B. Wie and Q. Liu, "Comparison Between Robustified Feedforward and Feedback for Achieving Performance Robustness," *Journal of Guidance, Control and Dynamics*, Vol. 15, No.4, 1992, pp.935-943.

[12] Q. Liu and B. Wie, "Robust Time-Optimal Control of Uncertain Flexible Spacecraft," *Journal of Guidance, Control and Dynamics*, Vol. 15, No.3, 1992, pp.597-604.

[13] T.C. Anthony, B. Wie and S. Carroll, "Pulse Modulated Control Synthesis for a Flexible Spacecraft," *Journal of Guidance, Control and Dynamics*, Vol. 13, No.6, 1990, pp.1014–1022.

[14] W.E. Vander Velde and J. He, "Design of Space Structure Control Systems Using On-Off Thrusters," *Journal of Guidance, Control and Dynamics*, Vol. 6, Jan-Feb, 1983, pp. 53–60.

[15] M.A. Floyd, M.E. Brown, J.D. Turner, and W.E. Vander Velde, "Implementation of a Minimum Time and Fuel On-Off Thruster Control System for Flexible Spacecraft," AAS/AIAA Astrodynamics Conference, Paper 83-376, Lake Placid, New York, August 22-25, 1983.

[16] M.L. de Oliveira e Souza, "Exactly Solving the Weighted Time/Fuel Optimal Control of an Underdamped Harmonic Oscillator," *Journal of Guidance, Control and Dynamics*, Vol. 11, No. 6 1988, pp. 488–494.

[17] B. Wie and C.T. Plescia, "Attitude Stabilization of a Flexible Spacecraft During Stationkeeping Maneuvers," *Journal of Guidance, Control and Dynamics*, Vol. 7. No. 4, 1984, pp.430–436.

[18] P. E. Gill, W. Murray, M. A. Saunders and M. H. Wright," Model Building and Practical Aspects of Nonlinear Programming", in Computational Mathematical Programming(ed. by K. Schittkowski), NATO ASI Series, 15, 1985, Springer Verlag, Berlin Germany.

[19] J. Stoer ,"Principles of Sequential Quadratic Programming Methods for Solving Nonlinear Programs", in Computational Mathematical Programming(ed. by K. Schittkowski) NATO ASI Series, 15, 1985, Springer Verlag, Berlin Germany.

[20] K.Schittkowski," On the Convergence of a Sequential Quadratic Programming Method with an Augmented Lagrangian Line Search Function", Mathematik Operationsforshung und Statistik, Serie Optimization, 14, 1983, pp197-216.

[21] K. Schittkowski," NLPQL : A FORTRAN Subroutine Solving Constrained Nonlinear Programming Problems", Annals of Operations Research (ed. Clyde L Monma), 5, 1986, pp485-500.

[22] J. J. Slotine, and S. S. Sastry, "Tracking Control of Nonlinear Systems Using Sliding Surfaces,with application to Robot Manipulators," *Int. Journal of Control*, Vol.38, No. 2, 1983, pp.465-492.

[23] J. J. Slotine, " Sliding Controller Design for Non-Linear Systems," *Int. Journal of Control*, Vol.40, No. 2, 1984, pp.421-434.

[24] V. I. Utkin, " Survey Paper- Variable Structure Systems Sliding Modes," *IEEE Trans. Automatic Control*, Vol.AC-22, No. 2, 1977, pp.212-222.

[25] B. R. Fernandez, and J. K. Hedrick, "Control of Multivariable Non-linear Systems by Sliding Mode Method," *Int. Journal of Control*, 1987, Vol.46, No. 3, pp.1019-1040 .

[26] B. Wie and D. Bernstein, "Benchmark Problems for Robust Control Design(1992 ACC Version)," *Proc. of the 1992 American Control Conference*, 1992.

APPENDIX A

Numerical Solution of Nonlinear Constrained Optimization Problem

Appendix A

Numerical Solution of Nonlinear Constrained Optimization Problem

The constrained parameter optimization problem can be solved using numerical schemes[18]-[21]. The problem can be stated as

$$\begin{aligned} min \quad & f(x), \qquad x \in R^n \\ g_j(x) = 0, \quad & j = 1, \ldots, m_e \\ g_j(x) \geq 0, \quad & j = m_e + 1, \ldots, m \\ x_l \leq \quad & x \leq x_u \end{aligned} \tag{A.1}$$

where x_l and x_u are the lower and upper bounds of x respectively. It is also assumed that the functions are all continuously differentiable.

Let the current iterate be x_k and v_k be the corresponding approximation of optimal Lagrangian multiplier. The positive definite approximation of the Hessian, B_k, of the Lagrangian function

$$L(x, u) = f(x) - \sum_{j=1}^{m'} u_j g_j(x) \tag{A.2}$$

where $u = (u_1, \ldots, u_{m'})^T \in R^{m'}$. Let the value $m' = m + 2n$. Let the bounds of x be defined as

$$\begin{aligned} g_j(x) &= x^{(j-m)} - x_l^{(j-m)}, \quad j = m+1, \ldots, m+n \\ g_j(x) &= x_u^{(j-m-n)} - x^{(j-m-n)}, \quad j = m+n+1, \ldots, m' \end{aligned} \tag{A.3}$$

Linearizing the constraints of the optimization and minimizing quadratic approximation of the Lagrangian function as

$$\begin{aligned} min\ \frac{1}{2}d^T B_k d &+ \nabla f(x_k)^T d \qquad (A.4)\\ \nabla g_j(x_k)^T d + g_j(x_k) &= 0, j = 1, \ldots, m_e,\\ \nabla g_j(x_k)^T d + g_j(x_k) &\geq 0, j = m_e + 1, \ldots, m,\\ x_l - x_k \leq d \leq x_u - x_k & \end{aligned}$$

Let d_k be the solution and u_k be the corresponding vector of the Lagrangian multiplier.

$$x_{k+1} = x_k + \alpha_k d_k \qquad (A.5)$$

where α_k is the line search parameter such that it decreases the 'merit function'. However Eq. (A.4) may lead into a non-feasible problem but it may still be feasible due to linearization of the constraints. Also it needs the gradients of the constraints at each iteration. To avoid these problems Schittkowski proposes an augmented Lagrangian method using the an additional variable δ,

$$\begin{aligned} min\ \frac{1}{2}d^T B_k d &+ f(x_k)^T d + \frac{1}{2}\rho_k \delta^2 \qquad (A.6)\\ \nabla g_j(x_k)^T d &+ (1-\delta) g_j(x_k) \geq 0, j \in J_k\\ \nabla g_j(x_{k(j)})^T d &+ g_j(x_k) \geq 0, j \in K_k\\ x_l &\leq x \leq x_u\\ 0 \leq \delta \leq 1, & \end{aligned}$$

where

$$\begin{aligned} J_k &= \{1, \ldots, m_e\} \cup\\ &\quad \{j : m_e < j \leq m, g_j(x_k) \leq \epsilon \text{ or } v_j^{(k)} > 0\}, \qquad (A.7)\\ K - K &= \{1, \ldots, m\}/J_k \qquad (A.8) \end{aligned}$$

where ϵ is the accuracy required and ρ_k is the additonal parameter used to reduce the influence of δ on the solution. The matrix B_k update can be used from the BFGS update formula given by

$$\begin{aligned} B_{k+1} &= B_k + \frac{q_k q_k^T}{q_k^T q_k} - \frac{B_k p_k p_k^T B_k}{p_k^T B_k p_k} \\ p_k &= x_{k+1} - x_k \\ q_k &= \nabla f(x_{k+1})^T - \nabla f(x_k)^T \end{aligned} \tag{A.9}$$

The constraints are non-linear and the cost function is linear. The standard IMSL subroutine NCONF uses successive quadratic programming method to solve a general nonlinear programming problem. It requires the value of the constraints and their gradients at each iteration. This scheme uses an initial guess value and then iterates to converge to the solution. There are many local optimum solutions which are obtained by using different initial guesses. However the optimum solution is one which has optimal cost function amongst the local optimum solutions.